Title

Welcome pathogens: transient heat dampens immune responses to acibenzolar-*S*-methyl in apple plants

Authors

Erwan Chavonet[1,†], Bao-huynh Nguyen[1,†], Christelle Heintz[1], Raphaël Cournol[1], Jitka Široká[2], Ondřej Novák[2], Romain Larbat[1], Matthieu Gaucher[1], Marie-Noëlle Brisset[1], Florent Pantin[1,*], Alexandre Degrave[1,*]

[1]Institut Agro, Univ Angers, INRAE, IRHS, SFR QuaSav, 49000, Angers, France
[2]Laboratory of Growth Regulators, Institute of Experimental Botany of the Czech Academy of Sciences & Palacký University, Šlechtitelů 27, 78371 Olomouc, Czech Republic
[†]Co-first authors.
*Authors for correspondence:
Florent Pantin florent.pantin@institut-agro.fr
Alexandre Degrave alexandre.degrave@institut-agro.fr

Word counts for the main sections: 7 537
Number of figures: 10 (all in colour)
Number of tables: 0
Supporting information: 7 supplementary figures and 2 supplementary tables

Abstract

Climate change affects plant-pathogen interactions, with disease outcome varying depending on pathosystem and environmental scenario. In Arabidopsis, a thermo-sensitive module of salicylic acid (SA) signaling makes immunity vulnerable to heat. The potent resistance inducer acibenzolar-*S*-methyl (ASM), an SA analogue that up-regulates transcription of defense genes, could restore plant protection under heat but not core SA signaling. Here, we investigated how high temperature rewires the ASM-induced responses of the apple immune system. We treated apple plants with ASM under contrasting heatwave scenarios and subsequently exposed them to *Erwinia amylovora* (the fire blight bacterium) or *Venturia inaequalis* (the apple scab fungus) while monitoring gene expression. While pre-exposing apple plants to high temperature did not change their susceptibility to pathogens, it drove a loss of ASM-induced protection. Transcriptomic analysis revealed broad dampening of ASM-regulation upon high temperature, for a wide range of biological processes beyond defense. We uncovered thermo-sensitive "resistance" and "susceptibility" marker genes with ASM-responsiveness being critically vulnerable to heat. We concluded that exposure to heatwave prevents ASM from fully mounting its protective responses in apple, not only lowering defenses but also offering more favorable hosting conditions. Our work highlights plant immunity as the joint outcome of resistant and susceptible responses.

Key words

Acibenzolar-*S*-methyl (ASM), defenses, *Erwinia amylovora* (fire blight), heat, immunity, *Malus domestica* (apple), susceptibility, *Venturia inaequalis* (apple scab)

ORCIDs

Erwan Chavonet	0009-0006-4985-5255
Bao-huynh Nguyen	0009-0004-4221-2885
Jitka Široká	0000-0002-4988-2919
Ondřej Novák	0000-0003-3452-0154
Romain Larbat	0000-0002-9060-5040
Matthieu Gaucher	0000-0003-2730-0639
Marie-Noëlle Brisset	0000-0002-5139-3292
Florent Pantin	0000-0003-0636-1061
Alexandre Degrave	0000-0002-5642-3235

Summary Statement

We found that heatwaves “disarm” apple’s ability to mount an effective inducible-immunity response against two major diseases, fire blight and apple scab. Heatwaves not only prevent full expression of plant defenses, but also favor a physiological status that is beneficial to the pathogens.

Introduction

Climate change modifies the many interactions between plants and pathogens. The 'disease triangle' framework posits that successful disease establishment requires a virulent pathogen, a susceptible host plant and favorable environmental conditions (Stevens, 1960; Velásquez *et al.*, 2018; Roussin-Léveillée *et al.*, 2024). Changes in temperature, radiation, relative humidity, soil water content and atmospheric CO_2 concentration may all affect the physiology and development of plants and pathogens, either directly or through their mutual interaction. For instance, temperature elevation has profound effects on plants, triggering thermomorphogenesis (Quint *et al.*, 2016), acceleration of phenology and growth (Parent *et al.*, 2010), alteration of carbon balance (Vasseur *et al.*, 2011), tissue desiccation (Marchin *et al.*, 2022) or even burning (Coupel-Ledru *et al.*, 2024), depending on the range and duration of temperature increase, the genetic background and the influence of other environmental factors (Long & Ort, 2010). Temperature elevation may also affect different components of the plant immune system, either positively or negatively (Malamy *et al.*, 1992; Zhu *et al.*, 2010; Cheng *et al.*, 2013; Zhang *et al.*, 2017; Richard *et al.*, 2020; Qiu *et al.*, 2022; Kim *et al.*, 2022). In turn, temperature elevation largely affects the growth rate and virulence of microbes, resulting in positive or negative effects depending on the species and strain, with feedback from host responses (Velásquez *et al.*, 2018; Roussin-Léveillée *et al.*, 2024). Thus, warming may confer more or less chance to a given microbe to meet and infect a susceptible plant, depending on the pathosystem and the environmental scenario (Desaint *et al.*, 2021; Chaloner *et al.*, 2021).

Focusing on the model pathosystem *Arabidopsis thaliana* / *Pseudomonas syringae*, recent reports have established that plant immunity is vulnerable to heat (28–30°C), through a negative effect on salicylic acid (SA) – one of the major hormones of plant defense (Peng *et al.*, 2021). Such vulnerability arises from a thermosensitive pair of master transcription factors (CBP60g and its paralogue SARD1) that fails to induce the expression of SA biosynthesis genes upon heat, making host plants more susceptible (Huot *et al.*, 2017; Kim *et al.*, 2022; Shields *et al.*, 2025). From the pathogen's perspective,

105 elevated temperature also enhances virulence by accelerating translocation of bacterial
106 effector proteins, leading to more severe disease under heat (Huot *et al.*, 2017). However,
107 over- or targeted- expression of *CBP60g* is sufficient to restore thermo-resilient SA
108 production and effective defense (Kim *et al.*, 2022), which suggests that loss of host SA
109 synthesis is the major driver of enhanced disease under heat within this pathosystem.
110 Application of acibenzolar-*S*-methyl (ASM, also known as BTH) effectively prevents
111 bacterial infection at warm temperature but, interestingly, does not restore the SA pathway
112 (Huot *et al.*, 2017). ASM is a long-standing plant resistance inducer that is converted *in*
113 *planta* into acibenzolar, a biologically active form that shares functional and structural
114 analogies with SA (Görlach *et al.*, 1996; Canet *et al.*, 2010a; Tripathi *et al.*, 2010). While
115 free or bound SA may accumulate upon ASM application in some species and
116 environmental conditions (e.g. Kuźniak *et al.*, 2014; Huot *et al.*, 2017; Ullah *et al.*, 2019;
117 Ratchaseema *et al.*, 2021), there is clear evidence that SA accumulation is dispensable
118 for efficient ASM-induced protection (Friedrich *et al.*, 1996; Lawton *et al.*, 1996; Canet *et*
119 *al.*, 2010a; Huot *et al.*, 2017). By contrast, ASM-induced protection critically requires
120 NPR1 (NONEXPRESSER OF PR GENES 1; Lawton *et al.*, 1996; Canet *et al.*, 2010a,b;
121 Huot *et al.*, 2017), now known as the SA receptor acting as a transcriptional co-activator
122 (Ding *et al.*, 2018). It is therefore likely that NPR1 directly recognizes acibenzolar to
123 activate downstream defense genes such as the canonical SA marker *PR1*
124 (*PATHOGENESIS-RELATED GENE 1*). In Arabidopsis at elevated temperature, applying
125 ASM properly initiates NPR1 signaling and yet fails to induce *PR1* expression and
126 feedforward SA accumulation (Huot *et al.*, 2017). This suggests that ASM can
127 counterbalance heat-sensitive immunity via other routes than the core SA pathway.
128
129 It is noteworthy, yet, that ASM regulates the transcription of hundreds of genes with
130 biological roles beyond defense, for instance by down-regulating genes related to
131 metabolism, photosynthesis or cell division (Huot *et al.*, 2017; Warneys *et al.*, 2018).
132 Among these processes that are routinely sustained by plants for their physiology and
133 development, some may involve susceptibility factors that are exploited by pathogens to
134 facilitate colonization and propagation *in planta* (Eckardt, 2002; van Schie & Takken,
135 2014; Gorshkov & Tsers, 2022). Thus, it is perhaps useful to consider plant immunity as

136 the joint outcome of resistant (R) and susceptible (S) responses. In this framework, ASM-
137 induced immunity would result from both the enhancement of defense genes and the
138 repression of susceptibility genes, with different effects on immunity, physiology and
139 development, depending on the species and the environment. To what extent high
140 temperature may affect the different components of ASM-induced immunity remains
141 largely unexplored.
142
143 We addressed this question on apple (*Malus domestica*), where ASM effectively controls
144 immunity by eliciting the production of defense compounds such as pathogenesis-related
145 (PR) proteins, and promotes resistance against several pests (Brisset *et al.*, 2000;
146 Maxson-Stein *et al.*, 2002; Dugé de Bernonville *et al.*, 2014; Aćimović *et al.*, 2015;
147 Marolleau *et al.*, 2017; Warneys *et al.*, 2018; Chavonet *et al.*, 2022). These include *Erwinia*
148 *amylovora*, a bacteria responsible for fire blight (Vanneste, 2000), and *Venturia*
149 *inaequalis*, a fungus responsible for apple scab (Bowen *et al.*, 2011). Both pathogens
150 exclusively infect young organs, yet their infection routes and pathogenic mechanisms
151 differ. Following penetration through natural pores or wounds of young leaves or flowers,
152 *E. amylovora* colonizes host apoplast by feeding on intracellular content spilling out from
153 cell death induced by bacterial type III effectors (Zeng *et al.*, 2021) and causes progressive
154 necrosis along the stem – potentially leading to tree death. Exudation of ooze droplets
155 from infected tissues is responsible for secondary infections. By contrast, germ tubes from
156 ascospores of *V. inaequalis* penetrate the cuticle of developing leaves or fruits, either
157 directly or through an appressorium, before forming stromata that extract plant nutrients
158 from the subcuticular space. Stromata then produce conidia that are spread by wind and
159 rain, originating secondary infections that occur throughout fruit development, leading to
160 necrotic lesions that render the fruits unmarketable (Bowen *et al.*, 2011). Most commercial
161 apple cultivars are susceptible to *E. amylovora* (Kostick *et al.*, 2019) and *V. inaequalis*
162 (Gessler *et al.*, 2006; Holb, 2007). The application of resistance inducers such as ASM is
163 a promising strategy to manage the protection of susceptible orchards against these two
164 diseases at least. Nonetheless, the efficacy of resistance inducers depends on
165 environmental conditions (Walters *et al.*, 2005, 2013; Sandroni *et al.*, 2020) – and the
166 components of immunity that are susceptible to the environment remain to be identified.

167

168 Here, we found that the efficacy of ASM protection against *E. amylovora* and *V. inaequalis*
169 erodes when apple plants are pre-exposed to transient heat. Such vulnerability to heat
170 was not accompanied by misregulation of master defense modules, contrasting with
171 Arabidopsis. Instead, transcriptomic analyses revealed that transient heat triggered
172 pervasive dampening of ASM-induced transcriptional regulation on a wide range of
173 physiological processes, leaving apple plants less immune. Thus, transient heat 'imprints'
174 the physiology of apple plants so that ASM-induced immunity becomes less protective
175 against pathogens in these conditions.

176

177 **Materials and Methods**

178

179 *Plant materials and growth conditions*

180 Experiments were performed on apple seedlings (3–6 leaves) obtained from seeds of
181 open-pollinated trees of cv. Golden Delicious, or on scions (2 to 6-month-old) of Golden
182 Delicious doubled-haploid 13 (GDDH13; Daccord *et al.*, 2017) grafted on the MM106
183 rootstock. Plants were cultivated in semi-controlled greenhouse conditions (natural
184 photoperiod supplemented with artificial light to reach a 16-h photophase, 23–25°C day,
185 17°C night, watering every 2–4 days) in individual pots filled with a growing medium
186 (Neuhaus Huminsubstrat N4, Klasmann-Deilman France, Bourgoin-Jallieu, France). Both
187 seedlings and grafted plants were chosen for protection experiments because of their
188 overall susceptibility to fire blight and apple scab, and transcriptomic analyses were
189 conducted on GDDH13 grafted scions to take advantage of the high-quality genome
190 sequence of this homozygous genotype (Daccord *et al.*, 2017). In all experiments, the
191 youngest unfolded leaf at time of treatment application was identified by attaching a small
192 clip to the petiole just before spraying ASM or water.

193

194 *Temperature and chemical treatments*

195 Temperature scenarios were applied in environmental chambers FitoClima 600 (ARALAB,
196 Rio de Mouro, Portugal) with controlled temperature, relative humidity (RH) and radiation
197 provided by white, blue and red LED tubes. In a first set of experiments, plants were

198 exposed to constant temperature (20°C) and RH (60%) day and night (12-h photoperiod
199 at 300 µmol m^{-2} s^{-1}). Heat was imposed by switching temperature to 35°C during 24 h or
200 during the 12-h photophase, depending on the experiment as described in the Results
201 section. In the following experiments, the environmental scenarios were refined to match
202 natural fluctuations, based on the average temperature dynamics on the 11 hottest days
203 (peak at 34–36°C) between March and July 2016–2018 in an experimental orchard
204 (UE449 HORTI, INRAE, Beaucouzé, France) adjacent to our research center (Fig. S1). A
205 typical heat day was designed through piecewise linear approximation of temperature,
206 relative humidity and irradiance over time, with a 4-h heat plateau in the afternoon ("Short"
207 settings") to be compared to standard conditions for apple tree growth in the same French
208 area ("Control" settings") and to an artificially extended 12-h heatwave ("Long" settings)
209 (Fig. S2). Nighttime temperature was set at 18°C until 8:00 am, followed by a 2-h ramp
210 and a 12-h plateau at 21°C and 35°C for the "Control" and "Long" settings, respectively,
211 or a 6-h ramp and a 4-h plateau at 35°C for the "Short" setting. Finally, a 2-h ("Control"
212 and "Long") or a 6-h ("Short") decreasing ramp was applied to reach 18°C at midnight. To
213 match natural variations, RH was covaried with temperature, reaching 80%, 60% and 40%
214 when temperature was 18°C, 21°C and 35°C, respectively (Fig. S2). The same daily
215 fluctuations in radiation were applied to the three regimes, based on the radiation
216 measured in the orchard. Lighting progressively started at 8:00 am to reach
217 300 µmol m^{-2} s^{-1} between midday and 4:00 pm, and progressively declined to switch off
218 at 8:00 pm. The number of days of heat vs. control temperatures depended on the
219 objective of experiment, and each scenario is described in Results for each experiment.

220 Acibenzolar-*S*-methyl (ASM) solutions were prepared from the commercial product Bion®
221 50WG (Syngenta, Basel, Switzerland; 50% of ASM) in reverse osmosis water at 0.4 g L^{-1}.
222 The same water was systematically used as control. Aerial parts of plants were sprayed
223 until incipient runoff with a spray gun Aeryo-1.4 (Deltalyo, Mably, France) between
224 8:00 am and 10:00 am on the day selected for the treatment. The timing of treatment in
225 relation to temperature scenario depended on the experiment and is described in Results.

226

227 *Quantification of ASM in treated leaves*

228 The morning of the experiment, seedlings from the greenhouse were sprayed with ASM
229 (t_0) and immediately transferred in ARALAB chambers at 20°C or 35°C (60% RH,
230 300 µmol m^{-2} s^{-1} PAR). After 6 h, when all leaves were unequivocally dry, the youngest
231 unfolded leaf was harvested on 2 plants, rinsed 3 times in water, dried with paper towel,
232 pooled in an Eppendorf and frozen in liquid nitrogen. This protocol was repeated on the
233 leaf insertion rank immediately below. For each leaf rank and each temperature, 10
234 replicates were obtained. Pooled samples were crushed to a fine powder with mortar and
235 pestle. Fresh leaves powders (50 mg) were suspended in 500 µL of methanol spiked with
236 0.2 µg mL^{-1} of [$^2H_6$]ABA as internal standard. After 10 s vortexing, mixtures were stored
237 for 15 h at –20°C and then centrifuged at 10000 g for 10 min at 4°C. The supernatant was
238 collected and the pellet extracted a second time with 500 µL of methanol. The two
239 combined supernatants were then evaporated using a vacuum concentrator. Dried
240 extracts were resuspended in 200 µl of methanol, filtered (0.2 µm) and transferred to vials
241 before LC-MS analysis.
242 Chromatographic analyses were performed on a Vanquish Flex UHPLC system equipped
243 with a quaternary solvent manager, an autosampler and a temperature-controlled column.
244 ASM and metabolites contained in the extracts (1 µL) were separated on a HSS-T3
245 column (100 × 2.1 mm, 1.8 µm) (Waters, Milford, MA, USA) using a gradient of mobile
246 phase composed of water + 0.1% formic acid (A) and methanol + 0.1% formic acid (B) at
247 a flow rate of 300 µL min^{-1}. The samples were kept at 10°C and the column was
248 maintained at 25°C. The elution program consisted in a first 2-min step with 0% B, then a
249 linear ramp from 0% to 100% B in 18 min, followed by a 3-min step with 100% B, before
250 re-equilibrating the column in the initial conditions for 7 min. The samples were analyzed
251 randomly.
252 MS^1 detection was performed on a TSQ Quantis Plus™ (ThermoFisher Scientific,
253 Bremen, Germany) mass spectrometer in positive and negative electrospray ionization
254 (ESI) modes. The capillary voltages were set at 3 kV and 2.75 kV for positive and negative
255 modes, respectively. The source gases were set (in arbitrary unit min^{-1}) to 40 (sheath
256 gas), 10 (auxiliary gas) and 0 (sweep gas) and the vaporizer temperature was 280°C. Full
257 scan MS^1 spectra were acquired from 50 to 700 *m/z* with a scan rate of 1000 Da s^{-1}. ASM
258 was quantified in selective ion monitoring (SIM) mode by following ion at *m/z* 211 in

259 positive mode. Acibenzolar acid was monitored at *m/z* 179 in negative mode together with
260 the internal standard [$^2H_6$]ABA at *m/z* 269. ASM, acibenzolar acid and [$^2H_6$]ABA pure
261 standards eluted at 18.1 min, 14.1 min and 19.7 min, respectively, with the above-
262 mentioned conditions. ASM and acibenzolar acid quantities in dry laminas were
263 determined using respective standard curves. Control leaves were also harvested at t_0
264 (without any spray) from independent plants in the greenhouse, and all samples were
265 below the detection limit.
266
267 *Physiological measurements*
268 The morning of the experiment, each plant was first characterized in the greenhouse.
269 Stem height (from the cotyledon to the apical meristem) and lamina length (youngest
270 unfolded leaf, just identified using a clip) were measured using a ruler. Stomatal
271 conductance (g_s) of the clipped leaf and of the leaf immediately below (more mature and
272 less susceptible to *E. amylovora* and *V. inaequalis*) was determined using a porometer
273 (LI-600; Li-COR Inc., Lincoln, NE, USA). Plants were then treated with ASM or water (t_0)
274 and immediately placed in ARALAB chambers at 12-h photoperiod, 250–300 µmol m^{-2} s^{-1}
275 PAR, and 60% RH. Air temperature was maintained at either 20°C or 35°C for 24 h. g_s of
276 both leaves were measured again at 24, 48 and 72 h after treatment. Stem height and
277 lamina length of the clipped leaf were measured again at 72 h after treatment and absolute
278 elongation rates were computed as the difference between initial and final lengths divided
279 by the time interval.
280
281 *Pathogen strains and protection experiments*
282 Plants were inoculated by the CFBP1430 strain of *E. amylovora* (Paulin & Sampson,
283 1973). Inoculum was suspended at 10^8 cfu mL^{-1} in reverse osmosis water from an
284 exponential growth phase culture cultivated overnight at 26°C on solid King's B medium
285 (King *et al.*, 1954). Inoculation was carried out in greenhouse conditions (1 or 3 d following
286 ASM treatment for seedlings, and 3 d after ASM treatment for grafted plants), by cutting
287 two-thirds of the two youngest unfolded leaves (perpendicularly to the midrib) with scissors
288 previously dipped in the inoculum. Progressions of necroses from the inoculated leaves
289 to the stems, through the midrib and petiole, were assessed 21 or 28 d post-inoculation

290 (dpi) for seedlings or grafted plants, respectively. Disease incidence was calculated as
291 the percentage of diseased plants, considering that a plant was diseased when typical fire
292 blight necrosis reached the stem, whereas it was considered healthy if no necrosis
293 occurred or if necrosis was restricted to the inoculated leaf (including its petiole) at the
294 end of the experiment.

295 The *V. inaequalis* strain 104 (Guillaumès *et al.*, 1995) was prepared in reverse-osmosis
296 water from scabbed apple leaves previously stored at –80 °C. The suspension was
297 roughly filtered to remove debris, adjusted to a concentration of 1.5×10^4 conidia mL^{-1} and
298 sprayed onto apple seedlings until incipient runoff. To facilitate conidial germination and
299 fungus penetration, plants were then placed in a controlled environment room in the dark,
300 at 18°C and with humidity maintained above 90% for 48 h. Light was then switched on
301 (16-h photoperiod), and humidity reduced to 70% while temperature was maintained at
302 18°C. Symptoms were assessed 21 d after inoculation on the youngest unfolded leaf at
303 the time of ASM application. The proportion of leaf area affected by sporulating lesions
304 was scored according to a 7-category ordinal scale (Calenge *et al.*, 2004). Disease
305 incidence was calculated as the percentage of diseased plants, considering that a plant
306 was diseased when visible sporulation occurred on the target leaf (category > 0).

307 The numbers of independent trials and biological replicates are indicated in the figure
308 legends.

309

310 *Sampling for gene expression and protein analyses*

311 Sampling for gene expression or protein analysis was carried out by pooling the youngest
312 unfolded leaf (or its distal two-thirds cut out while inoculating *E. amylovora*) from 1 to 5
313 plants to form one replicate. Samples were immediately frozen in liquid nitrogen and
314 stored at -80°C before processing. For the retrospective transcriptional analysis, leaves
315 were individually sampled while inoculating with *E. amylovora*, and pooled *a posteriori*
316 depending on the healthy or diseased fate of their corresponding plant. This was done
317 through hierarchical clustering analysis based on symptom severity (necrosis length)
318 scored at 7, 14 and 21 d after inoculation, where the most distant groups were selected

319 to distinguish between healthy and diseased plants. The genetic material (Golden
320 Delicious seedling or GDDH13 grafted plants) as well as the number of biological
321 replicates and independent experiments are indicated in the figure legends.

322

323 *Microarray procedure*

324 Leaves were ground in fine powder (Retsch, Haan, Germany) and total RNA was
325 extracted from about 200 mg using the Nucleospin RNA Plant Kit (Macherey-Nagel,
326 Düren, Germany) according to the manufacturer's protocol. Samples purity and
327 concentration were assayed with the Agilent 2100 bioanalyzer system and the RNA 6000
328 Nano LabChip kit (Agilent Technologies, Waldbroon, Germany) according to the
329 manufacturer's recommendation. Two hundred ng of RNA were amplified and labelled as
330 described in Perrin *et al.* (2020). Labelled cDNA were prepared for hybridization according
331 to the manufacturer's procedure with the Gene Expression Hybridization Kit (Agilent,
332 Waldbronn, Germany) and the Hi-RPM gene Expression Hybridization Kits (Agilent,
333 Waldbronn, Germany) and hybridized on AryANE v1.1 slides (Agilent, design n°85275) in
334 incubation chambers for 17 h at 65°C. After washing, slides were scanned at 3 µm with
335 an Innoscan 710 using Innoscan v3.4.7 software (Innopsys, Carbonne, France).

336

337 *Transcriptional marker analysis*

338 Leaves were ground and total RNA were extracted as described above in the microarray
339 procedure, except that RNA purity and concentration were assessed with a NanoDrop
340 One (Thermo Fisher Scientific, Waltham, MA, USA). Reverse transcription (RT) and
341 quantitative polymerase chain reaction (qPCR) were performed as described in Chavonet
342 *et al.* (2022). The primers and their targets designed for this study are listed in Table S2;
343 while the remaining ones are described in Dugé de Bernonville *et al.* (2014). The relative
344 changes in gene expression were calculated using the $2^{-\Delta\Delta CT}$ method (Schmittgen & Livak,
345 2008) with normalization against three internal reference genes (Vandesompele *et al.*,
346 2002). The mean expression value calculated from samples obtained on water-treated
347 plants exposed to control temperature (or 3-d heatwave for the experiments on heat wave

duration and positioning) was used as the calibrator to compute the relative expression as $\log_2$ ratios.

Protein extraction, separation and immunodetection

Two hundred mg of deep-frozen leaf powder were used for phenolic extraction of protein and their subsequent solubilization, as described in Chavonet *et al.* (2022). Ten µg of total protein extracts were separated on 1D SDS-PAGE, electroblotted onto 0.45 mm polyvinylidene difluoride (PVDF) membranes (immobilon-P, Milli- pore Corp., Bedford, MA, United States) as described in Warneys *et al.* (2018). Immunodetection of target proteins was performed using the rabbit primary antibodies described in Chavonet *et al.* (2022) using the procedure from Warneys *et al.* (2018).

Quantification of salicylates

Salicylic acid (SA), SA glucoside (SAG) and SA glucose ester (SGE) in laminas of apple seedlings were quantified in precisely weighed freeze-dried samples (1.8 ± 0.02 mg DW). Samples were extracted in 1 mL of 1 mol L^{-1} formic acid in 10% aqueous methanol with a stable isotope-labeled internal standard ([$^2H_4$]SA at 20 pmol per sample), following Široká *et al.* (2022). Extracts were purified with HLB Oasis® SPE columns (Waters) as described by Floková *et al.* (2014). SA was analysed on an Agilent 1290 Infinity LC system coupled to a 6490 Triple Quadrupole LC/MS, following Široká *et al.* (2022). SAG and SGE were determined from the same samples on an ACQUITY UPLC H-Class PLUS system linked to a Xevo TQ-S micro triple-quadrupole MS (Waters), operating in negative ionization multiple reaction monitoring mode (quantification: 299 > 137, collision energy 12 eV, cone voltage 30 V; confirmation: 299 > 93, collision energy 34 eV, cone voltage 28 V). Separation was performed on an Acquity UPLC BEH Shield C18 column (2.1 × 150 mm, 1.7 µm, Waters) at 40°C. The mobile phase consisted of 0.3% aqueous formic acid (A) and methanol (B), with a flow rate of 0.3 mL min^{-1} and a linear gradient from 5% to 98% B within 10 min. The determination of SAG and SGE was semi-quantitative, using [$^2H_4$]SA as internal standard.

Data analysis

Data analysis was performed using R (version 4.2.0; R Development Core Team, 2025) and RStudio (version 2024.09.0; R Studio Team, 2025) software except for Clustering Affinity Search Technique (CAST). Multiple comparisons on proportion of diseased and healthy plants were performed using pairwise Fisher's exact tests of the "rstatix" package (version 0.7.2; Kassambara, 2023a). Two-way ANOVA and estimation of the effect sizes (partial eta squared, η^2_p) of individual factors (treatment and temperature) and their interaction were performed using the same package. Multiple comparisons on expression values were performed with a Tukey's HSD test from package "stats" (R Development Core Team, 2025). Multiple comparisons on growth and conductance data were performed with pairwise t-tests adjusted by the Bonferroni method using "rstatix" (Kassambara, 2023a). Statistical differences for multiple comparisons were established with a risk threshold of 5% designated by different letters using package "rcompanion" (version 2.4.36; Mangiafico, 2024). For microarrays, data normalization and statistical analyses were performed using the LIMMA 3.10.1 package (Smyth, 2005) from the Bioconductor project, following Celton *et al.* (2014). Briefly, after extraction of the scan values with Mapix (version 8.2.5; Innopsys, Carbonne, France), the data were normalized with the lowess method, and differential expression analyses were performed using the lmFit function and Bayes moderated t test. Genes were considered differentially expressed (DEGs) for |log2 ratios| ≥ 1 and p-value ≤ 0.05. Pathway enrichment analysis was performed on all genes dataset without applying filtering with the Gene Set Enrichment Analysis (GSEA, 10000 permutations) by ranked genes by their $\log_2$ fold-change ratio (Subramanian *et al.*, 2005) with Benjamini and Hochberg procedure for controlling false discovery rate (Hung *et al.*, 2012), available with the package "ClusterProfiler" (version 4.4.4; Wu *et al.*, 2021). CAST was performed on genes corresponding to DEGs in at least one of the comparisons by the software MeV (Multi Experiment Viewer) with Pearson correlation distance metric and an affinity threshold of 0.95 (Ben-Dor *et al.*, 1999; Saeed *et al.*, 2003). Graphical representations were generated using the package "ggplot2" (version 3.5.1; Wickham, 2016) associated with "ggpubr" (version 0.6.0; Kassambara, 2023b). Heatmaps were performed with "ComplexHeatmap" (version 2.18.0; Gu, 2022). Principal Component Analysis (PCA) were carried out with

409 packages “FactoMineR” (version 2.8; Lê *et al.*, 2008) and “factoextra” (version 1.0.7;
410 Kassambara & Mundt, 2020).
411
412
413 **Results**
414
415 *High temperature impedes the protecting effect of ASM against fire blight and apple scab*
416
417 To explore the interaction between high temperature and ASM-induced immunity by
418 excluding any direct effect of temperature on pathogen growth or virulence, we targeted
419 ASM and/or heat applications prior to pathogen inoculation. We first sprayed apple
420 seedlings with ASM (or water) and immediately exposed them to a sudden temperature
421 elevation at 35°C during 24 h (or to a 20°C constant regime) as depicted in Fig. 1a (left
422 part). Transient heat and ASM treatments had no obvious impact on plant phenotype, as
423 illustrated by growth or stomatal conductance that remained unaffected (Fig. S3), either
424 on the youngest unfolded leaf at the time of ASM application (rank N) or in the leaf
425 immediately below (rank N-1). Three days after this dual prior treatment, when leaf N had
426 largely developed ontogenetic resistance, we inoculated the newly unfolded leaf (rank
427 N+1) with *E. amylovora* before assessing fire blight symptoms for three weeks. In control
428 conditions (water, 20°C), 82% of plants showed stem necrosis after 21 dpi (Fig. 1b). In
429 the ASM treatment, this proportion dropped to 50%. The variability in basal- and ASM-
430 induced- resistance, consistent with previous studies (Brisset *et al.*, 2000; Dugé de
431 Bernonville *et al.*, 2014; Chavonet *et al.*, 2022), could arise from inherent genetic variability
432 in the seedling population, gradients in the microclimate, and/or subtle differences in the
433 developmental stage of the inoculated leaf. High temperature *per se* did not enhance the
434 susceptibility of apple plants to fire blight in water-treated seedlings (Fig. 1b). However,
435 high temperature abolished the protecting effect of ASM that was observed at control
436 temperature, with 68% of plants showing stem necrosis. Similar results were obtained
437 when seedlings were exposed to a close environmental scenario and further inoculated
438 with *V. inaequalis* (Fig. 1c).
439

To check if this loss of ASM efficiency at high temperature could be observed in more realistic environmental conditions, we devised new scenarios based on records from a local meteorological station that corresponded to heatwave periods (Methods). We varied the duration of heat (numbers of days in the heatwave, and number of heat hours within a day) and inoculated the youngest unfolded leaf with *E. amylovora* systematically 1 d after ASM treatment (Fig. 2a). We found that applying a short heatwave with a 4-h plateau at 35°C during the photophase for 3 d induced a large loss of ASM-efficiency, similar to that in the previous experiment (Fig. 2b). Applying the same heatwave for only one day before inoculation was not sufficient to impede the effect of ASM. Nonetheless, when the heat plateau was extended to 12 h for a single day, ASM lost again most of its protecting effect. Altogether, these results show that accumulation of high temperatures prior to inoculation impairs the ability of apple plants to mount an effective ASM-induced protection against *E. amylovora* and *V. inaequalis*.

High temperature does not impair ASM uptake or SA metabolism

One trivial explanation might be that high temperature prevents correct uptake of ASM, due to e.g. enhanced evaporation and thus reduced leaf humectation. However, ASM content in treated leaves of apple seedlings 6 h after spraying (after complete evaporation) was similar at 20°C and 35°C (Fig. 3a). The quantity of ASM absorbed per leaf mass was similar between the youngest unfolded leaf (rank N) and the leaf immediately below (rank N-1), showing homogenous and efficient spray. Moreover, acibenzolar acid, the first catabolite of ASM that is biologically active (Tripathi *et al.*, 2010), was significantly enhanced at 35°C in both leaf ranks (Fig. 3b). This shows that ASM uptake and metabolism are operational at high temperature.

We also checked whether transient heat could alter SA metabolism, as observed in Arabidopsis (Huot *et al.*, 2017; Kim *et al.*, 2022). In apple seedlings exposed to control temperature, ASM did not induce SA accumulation 3 d after application, either in the youngest unfolded leaf at time of ASM spraying (Fig. 3c, rank N, left), or in the leaf above that had unfolded and was then inoculated (Fig. 3c, rank N+1, right). After 3 d again, the

471 inoculated leaf N+1 showed a large SA accumulation in both water- and ASM-treated
472 plants, consistent with a progression of the bacteria eliciting defense within the leaf
473 tissues, while the proximal, asymptomatic leaf N maintained a basal SA level (Fig. 3c).
474 Transient (24-h) exposure to heat did not affect SA content in water-treated plants the day
475 of inoculation, and ASM-treated plants tended to show enhanced SA, yet a large variability
476 was observed. Three days after inoculation, SA content in either leaf was not affected by
477 the prior temperature treatment. The conjugates SA glucoside (SAG) and SA glucose
478 ester (SGE) essentially showed the same variations as SA (Fig. 3d and e). Thus, there
479 was no apparent link between leaf SA content and ASM-induced protection.
480
481 *High temperature does not prevent ASM-induction of defense markers*
482
483 Our results on apple plants contrast with the Arabidopsis / *Pseudomonas syringae* model
484 pathosystem, where high temperature enhances plant susceptibility to the bacteria but
485 does not affect ASM-induced protection (Huot *et al.*, 2017). Nonetheless, in Arabidopsis
486 again, exposure to high temperature for 1 d before and after ASM application inhibits
487 ASM-induced expression of defense genes, including *PR1* (Huot *et al.*, 2017). Such
488 inhibition was also observed in rapeseed, tomato and rice (Kim *et al.*, 2022). Thus, high
489 temperature might prevent the transcriptional induction of defense genes by ASM in apple
490 plants, potentially underlying the loss of ASM-induced protection. To check this
491 hypothesis, we measured the expression of 29 marker genes covering a broad range of
492 defense mechanisms, including *PR1* (Dugé de Bernonville *et al.*, 2014; Chavonet *et al.*,
493 2022), on apple seedlings sprayed with ASM or water and exposed to transient heat or
494 not. Three days after ASM/water treatment, we sampled individual young leaves while
495 inoculating with *E. amylovora*, and kept track of whether the corresponding plants
496 remained healthy or turned diseased. Surprisingly, ASM efficiently induced the
497 transcription of defense markers whatever the temperature scenario, some of the genes
498 being even more induced by ASM at high temperature than at control temperature
499 (Fig. 4a). Thus, the transcriptional induction of defense marker genes by ASM was
500 uncoupled from plant protection at high temperature. Moreover, the expression profile of
501 defense markers at time of inoculation did not account for posterior disease symptoms,

502 as no major difference in gene transcription was observed in plants with healthy or
503 diseased fate (Fig. 4a). This suggests that transcriptional up-regulation of defense genes
504 at the infection site is necessary but not sufficient for effective immunity.
505 As translation can be poorly correlated with transcription during immune regulation (Xu et
506 al., 2017), we reasoned that high temperature may impede the translation of ASM-induced
507 transcripts. However, western blots performed on *MdAGG*, *MdPR2* and *MdPR10*, three
508 defense markers that had been previously associated with induced resistance at control
509 temperature (Chavonet *et al.*, 2022), revealed that protein accumulation was consistent
510 with gene expression (Fig. 4b and c). Overall, the loss of ASM efficiency at high
511 temperature was not captured by the variation of well-established defense markers, either
512 at the transcript or protein level.
513
514 *High temperature dampens transcriptomic response to ASM but does not repress global*
515 *defense*
516
517 To explore the broader changes in the transcriptional landscape induced by ASM and high
518 temperature, we performed a microarray analysis at the time of inoculation following a
519 three-day heatwave (Fig. 5a). For this purpose, we took advantage of the 'Golden
520 Delicious' doubled-haploid GDDH13 – the reference, homozygous apple genome
521 (Daccord *et al.*, 2017). We checked in GDDH13 grafted plants that high temperature also
522 induced a loss of ASM efficiency (Fig. S4), which was broadly similar to, yet less severe
523 than, the one observed in the seedlings of the 'Golden Delicious' progeny (Fig. 2b) –
524 thereby suggesting that genetics is not the major source of variability in our pathosystem.
525 We identified 3108 genes differentially expressed in at least one comparison (ASM vs.
526 water at a given temperature, or 35°C vs. 21°C for a given ASM or water treatment).
527 Overall, there was no strong transcriptomic effect of the prior heatwave for water-treated
528 plants (Fig. 5b). Comparatively, ASM triggered massive transcriptomic changes, with
529 patterns of up- and down-regulation that were largely conserved at both temperatures, yet
530 the magnitude of these changes compared to their respective water controls was globally
531 dampened at high temperature (Fig. 5b). GSEA analysis showed that ASM triggered
532 global up-regulation in processes such as response to biotic stimulus, response to stress,

533 signal transduction or alcohol metabolism, and down-regulation in processes such as cell
534 division, photosynthesis, lipid metabolism, cell wall organization or response to hormones
535 – at both temperatures (Fig. 5c). Interestingly, the functional categories for which up- or
536 down-regulation was most dampened at high temperature were not focused on defense,
537 but on cell division, signal transduction and various metabolic processes (Fig. 5c). Overall,
538 ASM induced large transcriptomic regulation that was softened at high temperatures for
539 some biological processes not obviously associated with defense.
540
541 *Dampening of ASM-induced transcriptional regulation at high temperature is partial but*
542 *pervasive*
543
544 To confirm the transcriptional signature of the ASM × temperature interaction, we selected
545 a set of representative genes for further RT-qPCR analyses on independent experiments.
546 For this purpose, we first performed Clustering Affinity Search Technique (CAST) on the
547 expression profiles of the 3108 genes that were differentially expressed in at least one
548 comparison, generating 26 clusters (Fig. S5; Table S1). Among those, five clusters (Fig.
549 6) were highlighted as they were reminiscent of reduced resistance (R) or increased
550 susceptibility (S) upon ASM application at high temperature, consistent with the
551 phenotypes. Two clusters gathered the majority of genes and reflected the previously
552 described global pattern, with an up- (cluster R1, 1130 genes) or down- (cluster S1, 1223
553 genes) regulation by ASM that is more or less dampened by high temperature. Such heat-
554 induced dampening was exacerbated in clusters R2 (187 genes) and S2 (102 genes),
555 respectively. Moreover, cluster R3 grouped 20 genes that were up-regulated by ASM at
556 control temperature but down-regulated by ASM at high temperature (R3). Overall,
557 clusters R1, R2 and R3 may be viewed as reservoirs of “resistance-associated genes”
558 expected to be up-regulated by ASM, while clusters S1 and S2 may contain “susceptibility-
559 associated genes” expected to be down-regulated by ASM – such up- or down-regulation
560 being potentially vulnerable to high temperature, especially in clusters R2, R3 and S2.
561 Supporting this classification, several PR-protein encoding genes were identified within
562 cluster R1, whereas two genes previously implicated in apple susceptibility to *E.*

563 *amylovora* (*DIPM3a* and *DIPM3b*; Meng *et al.*, 2006) were identified within cluster S1
564 (Table S1).
565
566 We selected 44 genes based on their distribution within these clusters and their functional
567 annotation, including genes putatively involved in defense processes, but also in
568 metabolism, cell cycle, transcription regulation, hormonal synthesis or cell wall properties
569 (Table S2). We designed primers that targeted these genes and also potentially their
570 homologues that were occasionally found across multiple clusters. As controls, we added
571 the three defense genes known for their strong up-regulation by ASM and monitored
572 previously: *MdAGG*, *MdPR2* and *MdPR10*. We then performed qPCR analyses that
573 globally confirmed the expected expression patterns, with a large effect of ASM and a
574 smaller effect of temperature (Fig. 7a). Consistent with this view, a PCA clearly separated
575 the genes based on their belonging to different cluster types ("resistance-associated" *vs*.
576 "susceptibility-associated"), and highlighted the major effect of ASM on gene expression
577 (Fig. 7b). While only a few genes showed significant ASM × temperature interaction (Fig.
578 7a), whereby high temperature restricts the up- or down-regulation induced by ASM, the
579 global interaction was evident on the PCA (Fig. 7b). This analysis confirms the partial but
580 broad-spectrum erosion, at high temperature, of ASM efficiency for transcription
581 regulation.
582
583 *Transcription regulation by ASM is more vulnerable to posterior heatwaves*
584
585 To further assess the vulnerability of ASM-induced transcriptional regulation to high
586 temperature, we varied the number of days (1 to 4) of plant exposure to heatwave, and
587 selected a subset of contrasting genes for qPCR analysis. The patterns of heat application
588 were designed so that i) ASM or water treatments were always applied at the beginning
589 of the last day of heatwaves, and ii) leaves were harvested at the same calendar time, 3 d
590 after the ASM/water treatment (Fig. 8a). The 3-d heatwave corresponded to the same
591 thermal regime as in the previous experiment, and the associated water treatment was
592 therefore selected for data calibration. Overall, the effect of ASM was larger than that of
593 the heatwave duration, and their interaction was minor (Fig. 8b). There was no obvious

594 dose-effect of the duration, which was difficult to interpret. Nonetheless, the transcriptional
595 effect of ASM towards “resistance-associated” markers (or away from “susceptibility-
596 associated” markers) was maximal for the 1-d heatwave, while the amplitude of response
597 to ASM was minimal for the 4-d heatwave (Fig. 8c). Thus, prolonged exposure to
598 heatwave tended to increase the vulnerability of ASM-induced transcriptional regulation,
599 yet the markers were not exquisitely sensitive to the heatwave duration when the
600 heatwave was applied before ASM application.
601
602 Finally, we varied the positioning of the heatwave in relation to the ASM application. A 3-
603 d heatwave was imposed just before, during (as in the previous experiments) or just after
604 the treatment application. Again, all GDDH13 leaves were harvested at the same calendar
605 time, 3 d after the ASM/water treatment (Fig. 9a). Gene up- or down-regulation by ASM
606 was more effective when the heatwave occurred before ASM application, and less
607 effective when it occurred afterward, as confirmed by significant interaction between ASM
608 and positioning (Fig. 9b) that was also evident in the PCA (Fig. 9c). A protection
609 experiment on seedlings against *E. amylovora* corroborated that ASM efficiency is higher
610 for a prior heatwave than for a posterior heatwave: when fire blight symptoms were scored
611 at 7, 14 or 21 dpi, the p-value of the ASM effect (Fisher’s exact test within each condition)
612 was always lower and around the significance threshold for a heatwave applied before
613 ASM (Fig. S6). These results suggest that high temperature does not prime apple plants
614 towards the erosion of ASM efficiency, but prevents ASM from mounting its full
615 transcriptional regulation straight away.
616
617
618 **Discussion**
619
620 Heatwaves are expected to become more prevalent with climate change and this may
621 affect plant immunity and pathogen virulence, with positive or negative impacts on disease
622 outcome depending on the pathosystem and the thermal scenario (Velásquez *et al.*, 2018;
623 Desaint *et al.*, 2021; Chaloner *et al.*, 2021; Roussin-Léveillée *et al.*, 2024). Here, we found
624 that subjecting apple plants to a short heatwave prior to infection with the bacteria *E.*

625 *amylovora* or the fungus *V. inaequalis* does not impact the development of disease
626 symptoms, but prevents ASM to drive an effective protection despite early accumulation
627 of acibenzolar and active SA metabolism. Our results suggest that pre-exposure to high
628 temperature affects ASM-induced immunity in apple plants, by preventing ASM from fully
629 regulating a wide array of genes that are not solely related to defense.
630
631 Vulnerability of immunity at high temperature in Arabidopsis is underpinned by a
632 temperature-susceptible module that normally drives the accumulation of SA and PR1
633 defense protein; however, ASM properly initiates NPR1-mediated signaling, and activates
634 other gene modules to drive effective resistance upon warm conditions (Huot *et al.*, 2017;
635 Kim *et al.*, 2022). In apple plants, we did not identify a major SA module vulnerable to high
636 temperature, but rather found that ASM-induced gene regulation was globally less efficient
637 following exposure to high temperature. Arabidopsis and other Brassicaceae mainly
638 synthesize SA through the isochorismate synthase (ICS) pathway that has evolved in this
639 family (Hong *et al.*, 2025), while most other plants would rely on the phenylalanine
640 ammonia-lyase (PAL) pathway (Hyun & Yoo, 2025). It is therefore plausible that thermo-
641 vulnerability of SA metabolism is specific to Bassicaceae's ICS pathway. The PAL
642 pathway has been very recently elucidated (Liu *et al.*, 2025; Wang *et al.*, 2025; Zhu *et al.*,
643 2025). Using our microarray data, we checked the pattern of the putative apple
644 orthologues of the newly identified genes, and found that ASM upregulates the expression
645 of several ones, especially at high temperature (Fig. S7), potentially explaining enhanced
646 salicylates in these conditions (Fig. 3c-e) – but obviously not the loss of ASM-induced
647 protection. Beyond SA metabolism, ASM normally rewires gene transcription so that
648 defense responses are up-regulated while growth-associated processes are down-
649 regulated (Huot *et al.*, 2017; Warneys *et al.*, 2018), which we confirmed here. At high
650 temperature, ASM triggered changes in the transcriptome that were essentially similar to
651 the ones at control temperature, yet attenuated. Overall, plants exposed to high
652 temperature and treated with ASM showed a transcriptomic signature evocative of lower
653 defense and higher susceptibility compared to ASM-treated plants at control temperature
654 (Fig. 10). The mechanisms by which high temperature eventually suppresses ASM-
655 induced protection in apple plants may therefore involve many end-players that each

656 partly contributes to plant resistance or susceptibility. For instance, heat stress partially
657 impaired ASM-induction of downstream resistance end-players with established roles
658 against different pests. These included e.g. *PR-10* (*PATHOGENESIS RELATED-10*),
659 homologues of ribonuclease proteins that possess antimicrobial properties (Liu &
660 Ekramoddoullah, 2006); *BIS2* (*BIPHENYL SYNTHASE 2*), enzymes involved in
661 biosynthesis of biphenyl and dibenzofuran phytoalexins in apple shoots, with antimicrobial
662 activity against *E. amylovora* (Chizzali *et al.*, 2012) and *V. inaequalis* (Hrazdina *et al.*,
663 1997); or *TPS4* (*TERPENE SYNTHASE 4*), enzymes that participate in the synthesis of
664 defensive volatile compounds in apple (Nieuwenhuizen *et al.*, 2013) such as (*E*,*E*)-α-
665 farnesene, a sesquiterpene repellent against rosy apple aphid (*Dysaphis plantaginea*;
666 Warneys *et al.*, 2018). Thus, ASM-induced resistance was transcriptionally compromised
667 by heat, correlating here with a loss of protection against *E. amylovora* and *V. inaequalis*.
668
669 Conversely, ASM may normally repress susceptibility or *S* genes that facilitate
670 compatibility with the pathogen, and fails to do so after heat stress, resulting in enhanced
671 plant susceptibility. Only a handful of susceptibility genes are known for the apple / *E.*
672 *amylovora* pathosystem, encoding apple proteins that interact with primary pathogenicity
673 effectors (Campa *et al.*, 2019; Pompili *et al.*, 2020; Tegtmeier *et al.*, 2020), while none
674 have been formally described for *V. inaequalis* so far. Our transcriptomic results support
675 the view that heat stress dampens ASM-driven down-regulation of some of these *S* genes.
676 Further *S* genes likely remain to be discovered, including those related to host physiology
677 that may be required to allow sustained compatibility, as exemplified in other
678 pathosystems (van Schie & Takken, 2014). While our "susceptibility-associated" markers
679 cannot be defined as genuine *S* genes, their de-repression upon heat may enhance plant
680 susceptibility. These markers contained a number of genes plausibly associated with DNA
681 replication or integrity – based on their Arabidopsis homologs (i.e. *WEE1*, *RPA70*, *TK*,
682 *BRCA2*, *ATXR6* – see Table S2 for full gene names). Other markers were possibly linked
683 to cell wall properties (*FLA12*; MacMillan *et al.*, 2010), solute transport (*ENODL17*;
684 Denancé *et al.*, 2014), or cell death execution (*PLP9*; La Camera *et al.*, 2005, 2009),
685 providing a diversity of potential entries whereby pathogens may divert host physiology.
686 In this framework, the erosion of ASM-induced down-regulation of genes useful to plant

687 physiology under heat, combined with the reduced induction of defense mechanisms,
688 would be exploited by the pathogen – effectively leveraging both sides of the "growth–
689 defense tradeoff" (Huot *et al.*, 2014; Monson *et al.*, 2022).
690
691 High temperature seems therefore to directly impede the transcriptional responses to
692 ASM. In line with this idea, the dampened transcriptional pattern was exacerbated when
693 positioning a 3-d heatwave just after the ASM treatment, i.e. when ASM-induced
694 transcription is fully active (Warneys *et al.*, 2018; Chavonet *et al.*, 2022). The molecular
695 mechanisms that link high-temperature perception to transcriptional regulation are
696 increasingly well-described, with the recent discovery of several plant thermosensors
697 (Casal *et al.*, 2024). Interestingly, the thermosensor THERMO-WITH ABA-RESPONSE 1
698 (TWA1) is a predicted intrinsically disordered protein that changes its conformation upon
699 high temperature, allowing physical interaction with the JASMONATE-ASSOCIATED
700 MYC2–LIKE 2 (JAM2) transcription factor and the TOPLESS (TPL) transcriptional
701 repressor, which down-regulates the expression of target genes and optimizes heat stress
702 response (Bohn *et al.*, 2024). JAM2 is a negative regulator of JA signaling (Sasaki-
703 Sekimoto *et al.*, 2013), a hormonal pathway that is down-regulated by *E. amylovora* during
704 the infection of susceptible apple plants (Dugé de Bernonville *et al.*, 2012). Moreover, the
705 classical JA–SA antagonism in Arabidopsis may turn into synergism under warm
706 conditions (Roussin-Léveillée *et al.*, 2024), due to a tunable regulation loop in the
707 expression of SA biosynthesis genes by JA (Mine *et al.*, 2017). This illustrates potential
708 connections between high temperature sensing and response to biotic cues through
709 transcriptional regulation. It should be stressed, however, that dampening of
710 transcriptional regulation was far from complete, suggesting that the loss of ASM-induced
711 protection at high temperature involves additional layers of biological modifications that
712 are not fully captured by transcripts. Tracking ASM-induced changes in the metabolome
713 upon high temperature could improve our understanding of the mechanisms underlying
714 the loss of protection we report.
715
716 In conclusion, our study unveils a loss of ASM-induced protection against fire blight and
717 apple scab upon transient exposure to heat stress. It covaries with a pervasive dampening

of ASM-induced transcription – and probably further physiological rearrangements – so that high temperature makes ASM-treated plants globally less capable of producing defense-related compounds toxic to microbes, and more prone to accumulate susceptible factors that facilitate microbial colonization. As plant response to ASM involves the regulation of many biological processes beyond defense, the protection efficacy of ASM is shaped by the environment due to the interplay between defense and physiology in plants. Disentangling this relationship would enhance our basic understanding of plant immunity in a changing climate, and may offer prospects for stabilizing the efficacy of plant resistance inducers in the field.

Acknowledgments

We thank Anthony Juillard, Brice Marolleau and Mylène Ruh for their involvement in disease assessment assays, the platforms ANAN (analysis of nucleic acids), PHYTO (Phytochemical analyses) and PHENOTIC (Angers Plant Phenotyping Facility, https://doi.org/10.17180/YKBZ-2V85) of the SFR QUASAV for excellent technical assistance, and the UE Horti (https://doi.org/10.15454/1.5573931618268674E12) for the supply of scions. This research was conducted in the framework of i) the regional program “Objectif Végétal, Research, Education and Innovation in Pays de la Loire”, supported by the French Region Pays de la Loire, Angers Loire Métropole and the European Regional Development Fund, ii) the France Agrimer Connaissances Program managed by the French Ministry of Agriculture (Project FAM-Connaissances 2023-11429220-OCASE) and iii) the French Priority Research Programme "Cultiver et Protéger Autrement" (PPR-CPA) managed by the Agence Nationale de la Recherche (project ANR-20-PCPA-0003 CapZeroPhyto). This work was also supported by the Czech Science Foundation (GACR) project No. 22-17435S, and by grants from the Ministère de l’Education Nationale, de l’Enseignement Supérieur et de la Recherche, France (to E.C.) and from INRAE-AGROECOSYSTEM Department and the Region Pays de la Loire, France (to B-h.N.). B-h.N. received a travel grant from VAAME Doctoral School for a stay in the Laboratory of Growth Regulators.

Competing interests

None declared.

Author contributions

A.D., F.P., M.G., R.L. and M.-N.B. conceived the project and designed the research plan. E.C. and B.-h.N. performed most of the experiments, with the contribution of R.C. and C.H. for some experiments. J.Š. and O.N. supervised hormonal analyses. A.D., F.P., M.G., R.L., M.-N.B., E.C. and B.-h.N. analyzed the data and wrote the manuscript. All authors read and approved the final manuscript.

Data availability

The microarray data sets presented in this study can be found in online repositories. The names of the repository and accession number can be found at: https://www.ncbi.nlm.nih.gov/geo/query/acc.cgi?acc=GSE280234.

References

Aćimović SG, Zeng Q, McGhee GC, Sundin GW, Wise JC. **2015**. Control of fire blight (*Erwinia amylovora*) on apple trees with trunk-injected plant resistance inducers and antibiotics and assessment of induction of pathogenesis-related protein genes. *Frontiers in Plant Science* **6**: 16.

Ben-Dor A, Shamir R, Yakhini Z. **1999**. Clustering gene expression patterns. *Journal of Computational Biology* **6**: 281–297.

Bohn L, Huang J, Weidig S, Yang Z, Heidersberger C, Genty B, Falter-Braun P, Christmann A, Grill E. **2024**. The temperature sensor TWA1 is required for thermotolerance in *Arabidopsis*. *Nature* **629**: 1126–1132.

Bowen JK, Mesarich CH, Bus VGM, Beresford RM, Plummer KM, Templeton MD. **2011**. *Venturia inaequalis*: the causal agent of apple scab. *Molecular Plant Pathology* **12**: 105–122.

783 **Brisset M-N, Cesbron S, Thomson SV, Paulin J-P**. **2000**. Acibenzolar-S-methyl induces the accumulation
784 of defense-related enzymes in apple and protects from fire blight. *European Journal of Plant Pathology* **106**:
785 529–536.

786 **Calenge F, Faure A, Goerre M, Gebhardt C, Van de Weg WE, Parisi L, Durel C-E**. **2004**. Quantitative
787 trait loci (QTL) analysis reveals both broad-spectrum and isolate-specific QTL for scab resistance in an
788 apple progeny challenged with eight isolates of *Venturia inaequalis*. *Phytopathology* **94**: 370–379.

789 **Campa M, Piazza S, Righetti L, Oh C-S, Conterno L, Borejsza-Wysocka E, Nagamangala KC, Beer**
790 **SV, Aldwinckle HS, Malnoy M**. **2019**. *HIPM* is a susceptibility gene of *Malus* spp.: Reduced expression
791 reduces susceptibility to *Erwinia amylovora*. *Molecular Plant-Microbe Interactions* **32**: 167–175.

792 **Canet JV, Dobón A, Ibáñez F, Perales L, Tornero P**. **2010a**. Resistance and biomass in Arabidopsis: a
793 new model for Salicylic Acid perception. *Plant Biotechnology Journal* **8**: 126–141.

794 **Canet JV, Dobón A, Roig A, Tornero P**. **2010b**. Structure-function analysis of *npr1* alleles in Arabidopsis
795 reveals a role for its paralogs in the perception of salicylic acid. *Plant, Cell & Environment* **33**: 1911–1922.

796 **Casal JJ, Murcia G, Bianchimano L**. **2024**. Plant thermosensors. *Annual Review of Genetics* **58**: 135–
797 158.

798 **Celton J-M, Gaillard S, Bruneau M, Pelletier S, Aubourg S, Martin-Magniette M-L, Navarro L, Laurens**
799 **F, Renou J-P**. **2014**. Widespread anti-sense transcription in apple is correlated with siRNA production and
800 indicates a large potential for transcriptional and/or post-transcriptional control. *New Phytologist* **203**: 287–
801 299.

802 **Chaloner TM, Gurr SJ, Bebber DP**. **2021**. Plant pathogen infection risk tracks global crop yields under
803 climate change. *Nature Climate Change* **11**: 710–715.

804 **Chavonet E, Gaucher M, Warneys R, Bodelot A, Heintz C, Juillard A, Cournol R, Widmalm G, Bowen**
805 **JK, Hamiaux C, *et al.* 2022**. Search for host defense markers uncovers an apple agglutination factor
806 corresponding with fire blight resistance. *Plant Physiology* **188**: 1350–1368.

807 **Cheng C, Gao X, Feng B, Sheen J, Shan L, He P**. **2013**. Plant immune response to pathogens differs with
808 changing temperatures. *Nature Communications* **4**: 2530.

809 **Chizzali C, Gaid MM, Belkheir AK, Hänsch R, Richter K, Flachowsky H, Peil A, Hanke M-V, Liu B,**
810 **Beerhues L**. **2012**. Differential expression of biphenyl synthase gene family members in fire-blight-infected
811 apple 'Holsteiner Cox'. *Plant Physiology* **158**: 864–875.

812 **Coupel-Ledru A, Westgeest AJ, Albasha R, Millan M, Pallas B, Doligez A, Flutre T, Segura V, This P,**
813 **Torregrosa L, *et al.* 2024**. Clusters of grapevine genes for a burning world. *New Phytologist* **242**: 10–18.

814 **Daccord N, Celton J-M, Linsmith G, Becker C, Choisne N, Schijlen E, van de Geest H, Bianco L,**
815 **Micheletti D, Velasco R, *et al.* 2017**. High-quality *de novo* assembly of the apple genome and methylome
816 dynamics of early fruit development. *Nature Genetics* **49**: 1099–1106.

817 **Denancé N, Szurek B, Noël LD**. **2014**. Emerging functions of nodulin-like proteins in non-nodulating plant
818 species. *Plant and Cell Physiology* **55**: 469–474.

819 **Desaint H, Aoun N, Deslandes L, Vailleau F, Roux F, Berthomé R**. **2021**. Fight hard or die trying: when
820 plants face pathogens under heat stress. *New Phytologist* **229**: 712–734.

821 **Ding Y, Sun T, Ao K, Peng Y, Zhang Y, Li X, Zhang Y**. **2018**. Opposite roles of salicylic acid receptors
822 NPR1 and NPR3/NPR4 in transcriptional regulation of plant immunity. *Cell* **173**: 1454-1467.e15.

Dugé de Bernonville T, Gaucher M, Flors V, Gaillard S, Paulin J-P, Dat JF, Brisset M-N. **2012**. T3SS-dependent differential modulations of the jasmonic acid pathway in susceptible and resistant genotypes of *Malus* spp. challenged with *Erwinia amylovora*. *Plant Science* **188–189**: 1–9.

Dugé de Bernonville T, Marolleau B, Staub J, Gaucher M, Brisset M-N. **2014**. Using molecular tools to decipher the complex world of plant resistance inducers: an apple case study. *Journal of Agricultural and Food Chemistry* **62**: 11403–11411.

Eckardt NA. **2002**. Plant disease susceptibility genes? *The Plant Cell* **14**: 1983–1986.

Floková K, Tarkowská D, Miersch O, Strnad M, Wasternack C, Novák O. **2014**. UHPLC–MS/MS based target profiling of stress-induced phytohormones. *Phytochemistry* **105**: 147–157.

Friedrich L, Lawton K, Ruess W, Masner P, Specker N, Gut Rella M, Meier B, Dincher S, Staub T, Uknes S, *et al.* 1996. A benzothiadiazole derivative induces systemic acquired resistance in tobacco. *The Plant Journal* **10**: 61–70.

Gessler C, Patocchi A, Sansavini S, Tartarini S, Gianfranceschi L. **2006**. *Venturia inaequalis* resistance in apple. *Critical Reviews in Plant Sciences* **25**: 473–503.

Görlach J, Volrath S, Knauf-Beiter G, Hengy G, Beckhove U, Kogel K-H, Oostendorp M, Staub T, Ward E, Kessmann H, *et al.* 1996. Benzothiadiazole, a novel class of inducers of systemic acquired resistance, activates gene expression and disease resistance in wheat. *The Plant Cell* **8**: 629–643.

Gorshkov V, Tsers I. **2022**. Plant susceptible responses: the underestimated side of plant–pathogen interactions. *Biological Reviews* **97**: 45–66.

Gu Z. **2022**. Complex heatmap visualization. *iMeta* **1**: e43.

Guillaumès J, Chevalier M, Parisi L. **1995**. Étude des relations *Venturia inaequalis* — *Malus* × *domestica* sur vitroplants. *Revue Canadienne de Phytopathologie* **17**: 305–311.

Holb IJ. **2007**. Classification of apple cultivar reactions to scab in integrated and organic production systems. *Canadian Journal of Plant Pathology* **29**: 251–260.

Hong K, Nakano M, Tang Y, Jeanguenin L, Kang W, Wang Y, Zuo L, Li P, He J, Jiang W, *et al.* 2025. Emergence of isochorismate-based salicylic acid biosynthesis within Brassicales. *Proceedings of the National Academy of Sciences of the United States of America* **122**: e2506170122.

Hrazdina G, Borejsza-Wysocki W, Lester C. **1997**. Phytoalexin production in an apple cultivar resistant to *Venturia inaequalis*. *Phytopathology* **87**: 868–876.

Hung J-H, Yang T-H, Hu Z, Weng Z, DeLisi C. **2012**. Gene set enrichment analysis: performance evaluation and usage guidelines. *Briefings in Bioinformatics* **13**: 281–291.

Huot B, Castroverde CDM, Velásquez AC, Hubbard E, Pulman JA, Yao J, Childs KL, Tsuda K, Montgomery BL, He SY. **2017**. Dual impact of elevated temperature on plant defence and bacterial virulence in *Arabidopsis*. *Nature Communications* **8**: 1808.

Huot B, Yao J, Montgomery BL, He SY. **2014**. Growth–defense tradeoffs in plants: a balancing act to optimize fitness. *Molecular Plant* **7**: 1267–1287.

Hyun J, Yoo H. **2025**. Missing steps uncovered in a pathway plants use to produce the defence molecule salicylic acid. *Nature* **645**: 48–50.

Kassambara A. **2023a**. rstatix: Pipe-friendly framework for basic statistical tests. R package version 0.7.2.

Kassambara A. **2023b**. ggpubr: 'ggplot2' based publication ready plots. R package version 0.6.0.

Kassambara A, Mundt F. **2020**. factoextra: Extract and visualize the results of multivariate data analyses. R package version 1.0.7.

Kim JH, Castroverde CDM, Huang S, Li C, Hilleary R, Seroka A, Sohrabi R, Medina-Yerena D, Huot B, Wang J, *et al.* 2022. Increasing the resilience of plant immunity to a warming climate. *Nature* **607**: 339–344.

King EO, Ward MK, Raney DE. **1954**. Two simple media for the demonstration of pyocyanin and fluorescin. *Journal of Laboratory and Clinical Medicine* **44**: 301–307.

Kostick SA, Norelli JL, Evans KM. **2019**. Novel metrics to classify fire blight resistance of 94 apple cultivars. *Plant Pathology* **68**: 985–996.

Kuźniak E, Głowacki R, Chwatko G, Kopczewski T, Wielanek M, Gajewska E, Skłodowska M. **2014**. Involvement of ascorbate, glutathione, protein S-thiolation and salicylic acid in benzothiadiazole-inducible defence response of cucumber against *Pseudomonas syringae* pv *lachrymans*. *Physiological and Molecular Plant Pathology* **86**: 89–97.

La Camera S, Balagué C, Göbel C, Geoffroy P, Legrand M, Feussner I, Roby D, Heitz T. **2009**. The *Arabidopsis* patatin-like protein 2 (PLP2) plays an essential role in cell death execution and differentially affects biosynthesis of oxylipins and resistance to pathogens. *Molecular Plant-Microbe Interactions* **22**: 469–481.

La Camera S, Geoffroy P, Samaha H, Ndiaye A, Rahim G, Legrand M, Heitz T. **2005**. A pathogen-inducible patatin-like lipid acyl hydrolase facilitates fungal and bacterial host colonization in Arabidopsis. *The Plant Journal* **44**: 810–825.

Lawton KA, Friedrich L, Hunt M, Weymann K, Delaney T, Kessmann H, Staub T, Ryals J. **1996**. Benzothiadiazole induces disease resistance in *Arabidopsis* by activation of the systemic acquired resistance signal transduction pathway. *The Plant Journal* **10**: 71–82.

Lê S, Josse J, Husson F. **2008**. FactoMineR: An R package for multivariate analysis. *Journal of Statistical Software* **25**: 1–18.

Liu J-J, Ekramoddoullah AKM. **2006**. The family 10 of plant pathogenesis-related proteins: Their structure, regulation, and function in response to biotic and abiotic stresses. *Physiological and Molecular Plant Pathology* **68**: 3–13.

Liu Y, Xu L, Wu M, Wang J, Qiu D, Lan J, Lu J, Zhang Y, Li X, Zhang Y. **2025**. Three-step biosynthesis of salicylic acid from benzoyl-CoA in plants. *Nature* **645**: 201–207.

Long SP, Ort DR. **2010**. More than taking the heat: crops and global change. *Current Opinion in Plant Biology* **13**: 240–247.

MacMillan CP, Mansfield SD, Stachurski ZH, Evans R, Southerton SG. **2010**. Fasciclin-like arabinogalactan proteins: specialization for stem biomechanics and cell wall architecture in Arabidopsis and *Eucalyptus*. *The Plant Journal* **62**: 689–703.

Malamy J, Hennig J, Klessig DF. **1992**. Temperature-dependent induction of salicylic acid and its conjugates during the resistance response to tobacco mosaic virus infection. *The Plant Cell* **4**: 359–366.

Mangiafico SS. **2024**. rcompanion: Functions to support extension education program evaluation. R package version 2.4.36.

Marchin RM, Backes D, Ossola A, Leishman MR, Tjoelker MG, Ellsworth DS. **2022**. Extreme heat increases stomatal conductance and drought-induced mortality risk in vulnerable plant species. *Global Change Biology* **28**: 1133–1146.

Marolleau B, Gaucher M, Heintz C, Degrave A, Warneys R, Orain G, Lemarquand A, Brisset M-N. **2017**. When a plant resistance inducer leaves the lab for the field: integrating ASM into routine apple protection practices. *Frontiers in Plant Science* **8**: 1938.

Maxson-Stein K, He S-Y, Hammerschmidt R, Jones AL. **2002**. Effect of treating apple trees with acibenzolar-*S*-methyl on fire blight and expression of pathogenesis-related protein genes. *Plant Disease* **86**: 785–790.

Meng X, Bonasera JM, Kim JF, Nissinen RM, Beer SV. **2006**. Apple proteins that interact with DspA/E, a pathogenicity effector of *Erwinia amylovora*, the fire blight pathogen. *Molecular Plant-Microbe Interactions* **19**: 53–61.

Mine A, Nobori T, Salazar-Rondon MC, Winkelmüller TM, Anver S, Becker D, Tsuda K. **2017**. An incoherent feed-forward loop mediates robustness and tunability in a plant immune network. *EMBO Reports* **18**: 464–476.

Monson RK, Trowbridge AM, Lindroth RL, Lerdau MT. **2022**. Coordinated resource allocation to plant growth–defense tradeoffs. *New Phytologist* **233**: 1051–1066.

Nieuwenhuizen NJ, Green SA, Chen X, Bailleul EJD, Matich AJ, Wang MY, Atkinson RG. **2013**. Functional genomics reveals that a compact terpene synthase gene family can account for terpene volatile production in apple. *Plant Physiology* **161**: 787–804.

Parent B, Turc O, Gibon Y, Stitt M, Tardieu F. **2010**. Modelling temperature-compensated physiological rates, based on the co-ordination of responses to temperature of developmental processes. *Journal of Experimental Botany* **61**: 2057–2069.

Paulin J-P, Sampson R. **1973**. Le feu bactérien en France. II. Caractères des souches d'*Erwinia amylovora* (Burrill), Winslow et al. 1920, isolées du foyer franco-belge. *Annales de Phytopathologie* **5**: 389–397.

Peng Y, Yang J, Li X, Zhang Y. **2021**. Salicylic acid: biosynthesis and signaling. *Annual Review of Plant Biology* **72**: 761–791.

Perrin A, Daccord N, Roquis D, Celton J-M, Vergne E, Bucher E. **2020**. Divergent DNA methylation signatures of juvenile seedlings, grafts and adult apple trees. *Epigenomes* **4**: 4.

Pompili V, Dalla Costa L, Piazza S, Pindo M, Malnoy M. **2020**. Reduced fire blight susceptibility in apple cultivars using a high-efficiency CRISPR/Cas9-FLP/FRT-based gene editing system. *Plant Biotechnology Journal* **18**: 845–858.

Qiu J, Xie J, Chen Y, Shen Z, Shi H, Naqvi NI, Qian Q, Liang Y, Kou Y. **2022**. Warm temperature compromises JA-regulated basal resistance to enhance *Magnaporthe oryzae* infection in rice. *Molecular Plant* **15**: 723–739.

Quint M, Delker C, Franklin KA, Wigge PA, Halliday KJ, Zanten M van. **2016**. Molecular and genetic control of plant thermomorphogenesis. *Nature Plants* **2**: 15190.

R Development Core Team. **2025**. R: A language and environment for statistical computing.

R Studio Team. **2025**. RStudio: Integrated development environment for R.

Ratchaseema MTN, Kladsuwan L, Soulard L, Swangmaneecharern P, Punpee P, Klomsa-ard P, Sriroth K, Keawsompong S. **2021**. The role of salicylic acid and benzothiadiazole in decreasing phytoplasma titer of sugarcane white leaf disease. *Scientific Reports* **11**: 15211.

Richard MMS, Knip M, Aalders T, Beijaert MS, Takken FLW. **2020**. Unlike many disease resistances, Rx1-mediated immunity to Potato Virus X is not compromised at elevated temperatures. *Frontiers in Genetics* **11**: 417.

Roussin-Léveillée C, Rossi CAM, Castroverde CDM, Moffett P. **2024**. The plant disease triangle facing climate change: a molecular perspective. *Trends in Plant Science* **29**: 895–914.

Saeed AI, Sharov V, White J, Li J, Liang W, Bhagabati N, Braisted J, Klapa M, Currier T, Thiagarajan M, *et al.* 2003. TM4: A free, open-source system for microarray data management and analysis. *BioTechniques* **34**: 374–378.

Sandroni M, Liljeroth E, Mulugeta T, Alexandersson E. **2020**. Plant resistance inducers (PRIs): perspectives for future disease management in the field. *CABI Reviews* **15**: 001.

Sasaki-Sekimoto Y, Jikumaru Y, Obayashi T, Saito H, Masuda S, Kamiya Y, Ohta H, Shirasu K. **2013**. Basic helix-loop-helix transcription factors JASMONATE-ASSOCIATED MYC2-LIKE1 (JAM1), JAM2, and JAM3 are negative regulators of jasmonate responses in Arabidopsis. *Plant Physiology* **163**: 291–304.

van Schie CCN, Takken FLW. **2014**. Susceptibility genes 101: how to be a good host. *Annual Review of Phytopathology* **52**: 551–581.

Schmittgen TD, Livak KJ. **2008**. Analyzing real-time PCR data by the comparative C_T method. *Nature Protocols* **3**: 1101–1108.

Shields A, Yao L, Rossi CAM, Collado Cordon P, Kim JH, AlTemen WMA, Li S, Marchetta EJR, Shivnauth V, Chen T, *et al.* 2025. Warm temperature suppresses plant systemic acquired resistance by intercepting *N*-hydroxypipecolic acid biosynthesis. *The Plant Journal* **123**: e70374.

Široká J, Brunoni F, Pěnčík A, Mik V, Žukauskaitė A, Strnad M, Novák O, Floková K. **2022**. High-throughput interspecies profiling of acidic plant hormones using miniaturised sample processing. *Plant Methods* **18**: 122.

Smyth GK. **2005**. limma: Linear models for microarray data. In: Gentleman R, Carey VJ, Huber W, Irizarry RA, Dudoit S, eds. Bioinformatics and Computational Biology Solutions Using R and Bioconductor. New York, USA: Springer, 397–420.

Stevens RB. **1960**. Chapter 10 - Cultural practices in disease control. In: Horsfall JG, Dimond AE, eds. Plant Pathology: An Advanced Treatise. New York and London: Academic Press, 357–429.

Subramanian A, Tamayo P, Mootha VK, Mukherjee S, Ebert BL, Gillette MA, Paulovich A, Pomeroy SL, Golub TR, Lander ES, *et al.* 2005. Gene set enrichment analysis: A knowledge-based approach for interpreting genome-wide expression profiles. *Proceedings of the National Academy of Sciences of the United States of America* **102**: 15545–15550.

Tegtmeier R, Pompili V, Singh J, Micheletti D, Silva KJP, Malnoy M, Khan A. **2020**. Candidate gene mapping identifies genomic variations in the fire blight susceptibility genes *HIPM* and *DIPM* across the *Malus* germplasm. *Scientific Reports* **10**: 16317.

Tripathi D, Jiang Y-L, Kumar D. **2010**. SABP2, a methyl salicylate esterase is required for the systemic acquired resistance induced by acibenzolar-*S*-methyl in plants. *FEBS Letters* **584**: 3458–3463.

Ullah C, Tsai C-J, Unsicker SB, Xue L, Reichelt M, Gershenzon J, Hammerbacher A. **2019**. Salicylic acid activates poplar defense against the biotrophic rust fungus *Melampsora larici-populina* via increased biosynthesis of catechin and proanthocyanidins. *New Phytologist* **221**: 960–975.

Vandesompele J, de Preter K, Pattyn F, Poppe B, van Roy N, de Paepe A, Speleman F. **2002**. Accurate normalization of real-time quantitative RT-PCR data by geometric averaging of multiple internal control genes. *Genome Biology* **3**: research0034.1-0034.11.

Vanneste JL (Ed.). **2000**. *Fire blight: the disease and its causative agent,* Erwinia amylovora. Wallingford, UK: CABI.

Vasseur F, Pantin F, Vile D. **2011**. Changes in light intensity reveal a major role for carbon balance in *Arabidopsis* responses to high temperature. *Plant, Cell & Environment* **34**: 1563–1576.

Velásquez AC, Castroverde CDM, He SY. **2018**. Plant–pathogen warfare under changing climate conditions. *Current Biology* **28**: R619–R634.

Walters DR, Ratsep J, Havis ND. **2013**. Controlling crop diseases using induced resistance: challenges for the future. *Journal of Experimental Botany* **64**: 1263–1280.

Walters D, Walsh D, Newton A, Lyon G. **2005**. Induced resistance for plant disease control: Maximizing the efficacy of resistance elicitors. *Phytopathology* **95**: 1368–1373.

Wang Y, Song S, Zhang W, Deng Q, Feng Y, Tao M, Kang M, Zhang Q, Yang L, Wang X, *et al.* 2025. Deciphering phenylalanine-derived salicylic acid biosynthesis in plants. *Nature* **645**: 208–217.

Warneys R, Gaucher M, Robert P, Aligon S, Anton S, Aubourg S, Barthes N, Braud F, Cournol R, Gadenne C, *et al.* 2018. Acibenzolar-*S*-methyl reprograms apple transcriptome toward resistance to rosy apple aphid. *Frontiers in Plant Science* **9**: 1795.

Wickham H. **2016**. *ggplot2: Elegant Graphics for Data Analysis*. New York, USA: Springer-Verlag.

Wu T, Hu E, Xu S, Chen M, Guo P, Dai Z, Feng T, Zhou L, Tang W, Zhan L, *et al.* 2021. clusterProfiler 4.0: A universal enrichment tool for interpreting omics data. *The Innovation* **2**: 100141.

Zeng Q, Puławska J, Schachterle J. **2021**. Early events in fire blight infection and pathogenesis of *Erwinia amylovora*. *Journal of Plant Pathology* **103**: 13–24.

Zhang W, Chen S, Abate Z, Nirmala J, Rouse MN, Dubcovsky J. **2017**. Identification and characterization of *Sr13*, a tetraploid wheat gene that confers resistance to the Ug99 stem rust race group. *Proceedings of the National Academy of Sciences of the United States of America* **114**: E9483–E9492.

Zhu Y, Qian W, Hua J. **2010**. Temperature modulates plant defense responses through NB-LRR proteins. *PLoS Pathogens* **6**: e1000844.

Zhu B, Zhang Y, Gao R, Wu Z, Zhang W, Zhang C, Zhang P, Ye C, Yao L, Jin Y, *et al.* 2025. Complete biosynthesis of salicylic acid from phenylalanine in plants. *Nature* **645**: 218–227.

1016 *Supporting Information*

1017

1018 Additional Supporting Information may be found online in the Supporting Information
1019 section at the end of the article.

1020

1021 **Figure S1.** Climatic variables measured at the meteorological station of Beaucouzé
1022 (France) for the eleven hottest days recorded between March 2016 and July 2018.
1023 **Figure S2.** Climate dynamics applied in the growth chamber to study the effect of
1024 heatwaves on apple response to ASM.
1025 **Figure S3.** Impact of heat and treatment on plant phenotype, and representative
1026 photographs of apple seedlings and their typical disease symptoms.
1027 **Figure S4.** Accumulation of high temperatures prior to inoculation impairs the ability of
1028 apple grafts of GDDH13 to mount an effective ASM-induced protection against *E.*
1029 *amylovora*.
1030 **Figure S5.** Identification of gene clusters by CAST.
1031 **Figure S6.** Protection provided by ASM to apple seedlings against *E. amylovora* is more
1032 strongly dampened by a heatwave posterior to ASM application than by a prior heatwave.
1033 **Figure S7.** Putative apple genes of SA biosynthesis pathway are induced by ASM at high
1034 temperature.
1035 **Table S1.** List of genes that are differentially regulated by ASM treatment and transient
1036 heat according to the microarray analysis.
1037 **Table S2.** Design of “resistance” and “susceptibility” marker genes.

1038

1039

1040 **Figures captions**

1041

1042 **Fig. 1. Protection provided by ASM to apple seedlings against *E. amylovora* and *V.***
1043 ***inaequalis* is impaired by transient exposure to heat. (a)** Schematic representation of
1044 the experimental protocol applied to plants for *E. amylovora* (left) and *V. inaequalis* (right)
1045 disease assessment (details in Methods). Plants were grown in a greenhouse (light blue)
1046 before being transferred in chambers for application of thermal scenario (dark blue to

1047 yellow color map depicting temperature). For inoculation and symptom assessment,
1048 plants returned to greenhouse conditions (*E. amylovora*), or moved to a controlled
1049 environment room at 18°C (*V. inaequalis*) in darkness during 2 d (dark gray) and then in
1050 normal light/dark cycles (light green). Arrows indicate the application of ASM (or water)
1051 treatment and pathogen inoculation on the youngest unfolded leaf. **(b)** Stacked bar chart
1052 showing the proportion of healthy (asymptomatic on stem) and diseased (symptomatic on
1053 stem) seedlings inoculated with *E. amylovora*, 21 d post-inoculation. **(c)** Stacked bar chart
1054 showing the proportion of healthy (no visible sporulation) and diseased (visible
1055 sporulation) seedlings inoculated with *V. inaequalis*, 21 d post-inoculation. Data represent
1056 78 to 85 biological replicates from 2 independent trials for each pathogen (n = total number
1057 of plants). Statistical significance was determined using pairwise Fisher's exact tests;
1058 same letters indicate groups that are not significantly different. Icons created in
1059 BioRender.com.
1060
1061 **Fig. 2. Accumulation of high temperatures prior to inoculation impairs the ability of**
1062 **apple seedlings to mount an effective ASM-induced protection against *E.***
1063 ***amylovora*. (a)** Schematic representation of the experimental protocol (details in
1064 Methods). Air temperature during the contrasting thermal scenario (period in the growth
1065 chamber) is color-coded according to the color map. Arrows indicate the application of
1066 ASM (or water) treatment and pathogen inoculation on the youngest unfolded leaf. **(b)**
1067 Stacked bar chart of seedlings showing the proportion of healthy (asymptomatic on stem)
1068 and diseased (symptomatic on stem) seedlings inoculated with *E. amylovora*, 21 d post-
1069 inoculation. Data represent 60 biological replicates from 3 independent trials (n = total
1070 number of plants). Statistical significance was determined using pairwise Fisher's exact
1071 tests; same letters indicate groups that are not significantly different. Icons created in
1072 BioRender.com.
1073
1074 **Fig. 3. High temperature does not alter ASM uptake or SA metabolism in apple**
1075 **seedlings. (a)** and **(b)** Content of ASM and acibenzolar acid (biologically-active
1076 catabolite) in the lamina of ASM-treated leaves (n = 10, each pooled from 2 different
1077 plants). Apple seedlings were sprayed with ASM (t_0) and immediately transferred into a

1078 chamber at 20°C or 35°C. The youngest fully unfolded leaf (rank N) and the leaf below
1079 (rank N-1) were sampled after 6 h (when the sprayed solution had evaporated) and
1080 thoroughly rinsed before quantification of **(a)** ASM and **(b)** acibenzolar acid. **(c)**, **(d)** and
1081 **(e)** Content of salicylates in the lamina of water- or ASM-treated leaves (n = 6, each pooled
1082 from 8 different plants). Apple seedlings were sprayed with water or ASM (t_0) and
1083 immediately transferred into a chamber at 20°C or 35°C for 24 h, before being placed in
1084 a greenhouse. Three days after spraying (t_0+3d), half of the plants was sampled for the
1085 youngest fully unfolded leaf at time of spraying (rank N) and the leaf above (rank N+1),
1086 while the other half was inoculated with *E. amylovora* at leaf N+1. At three days post-
1087 inoculation (3 dpi, t_0+6d), the inoculated leaf N+1 and leaf N were harvested. A batch of
1088 plants was also harvested for leaf N just before t_0, in the greenhouse where the seedlings
1089 were grown. The samples were quantified for **(c)** salicylic acid (SA), **(d)** SA glucoside
1090 (SAG) and **(e)** SA glucose ester (SGE). ns: not significant, *: P<0.05, **: P<0.01, ***:
1091 P<0.001, ****: P<0.0001.
1092
1093 **Fig. 4. High temperature does not prevent ASM-induction of defense markers. (a)**
1094 Retrospective transcriptional analysis of 29 marker genes covering a broad range of apple
1095 defense mechanisms. Following a scenario similar as in Fig. 1a, young leaves of apple
1096 seedlings were individually sampled while inoculating with *E. amylovora*, and grouped *a*
1097 *posteriori* depending on the healthy or diseased fate of their corresponding plant.
1098 Heatmaps show relative gene expression and ANOVA effect sizes (η^2_p) of treatment,
1099 temperature and their interaction, as well as their respective significance level (*P<0.05,
1100 **P<0.01, ***P<0.001, ****P<0.0001), for both types of plants. Expression values of the
1101 average of water-treated leaves from healthy and diseased plants exposed to 20°C were
1102 used for the calculation of the $\log_2$ ratio. Expression values were obtained from 5–9
1103 biological replicates (pools of 2 to 4 youngest unfolded leaves at time of ASM or water
1104 treatment) from a single trial. **(b)** Relative expression of *MdAGG*, *MdPR2* and *MdPR10*
1105 from two independent experiments performed in the same conditions as in Fig. 5a (3-d
1106 heatwave, GDDH13 grafted plants – see afterwards). The youngest unfolded leaf at time
1107 of sampling was collected from 5 plants per experiment. **(c)** Protein immunodetection of
1108 defense-associated proteins. Equal quantities (10 µg) of each protein sample were loaded

1109 and run in three separate SDS-PAGE gels. Following transfer to PVDF membranes, each
1110 blot was probed with the appropriate primary antibody to detect MdAGG, MdPR2, and
1111 MdPR10. Each sample corresponds to a pool of proteins extracted from the 5 biological
1112 replicates per experiment presented in **(b)**.
1113
1114 **Fig. 5. High temperature dampens transcriptomic response to ASM but does not**
1115 **repress global defense. (a)** Schematic diagram of the experimental protocol. Air
1116 temperature during the contrasting thermal scenario (period in the growth chamber) is
1117 color-coded according to the color map. Arrows indicate the application of ASM or water
1118 treatment and the sampling of the youngest unfolded leaf of GDDH13 grafted plants
1119 dedicated to microarray analysis. **(b)** Heatmap of 3108 DEGs identified in at least one
1120 microarray comparison. DEGs were defined by a $|\log_2 \text{ratio}| \geq 1$ and $P < 0.05$. The
1121 hierarchical clustering dendrogram was constructed from the dissimilarity matrix.
1122 Expression values were obtained from 2 biological replicates (each pooled from the
1123 youngest fully expanded leaf of 4 grafted plants) from 2 independent trials. **(c)** Ridgeline
1124 plot of GSEA on biological process ontology performed on comparison ASM/water for
1125 plants exposed to both 21°C and 35°C and 35°C/21°C comparison for ASM-treated plants.
1126 GSEA was obtained by 10.000 permutations with Benjamini and Hochberg procedure for
1127 p-value adjustment.
1128
1129 **Fig. 6. Identification of "resistance-associated" and "susceptibility-associated"**
1130 **marker genes by clustering.** CAST clustering performed on the 3108 DEGs (Table S1
1131 and Fig. S5) yielded several clusters evocative of resistant (R1, R2 and R3) and
1132 susceptible (S1 and S2) marker genes. The average pattern of expression ratio (± sd) is
1133 shown for each cluster. The number of DEGs in each resistance or susceptibility cluster
1134 are indicated in the upper right- or left-hand corner, respectively. To facilitate the
1135 interpretation of the variations in ratios, barplots showing the inferred expression pattern
1136 relative to the control (water, 21°C) are placed in the lower left- or right-hand corner of
1137 resistance and susceptibility clusters, respectively.
1138

1139 **Fig. 7. High temperature erodes ASM-induced transcriptional regulation of**
1140 **resistance- and susceptibility-associated marker genes.** Expression values of water-
1141 treated leaves from plants exposed to 21°C were used for the calculation of the log_2 ratio.
1142 Expression values were obtained from 10 biological replicates equally from 2 independent
1143 trials. **(a)** Heatmap showing relative gene expression and ANOVA effect sizes (η^2_p) of
1144 treatment, temperature and their interaction, as well as their respective significance level
1145 (*P<0.05, **P<0.01, ***P<0.001, ****P<0.0001). **(b)** PCA representation of relative gene
1146 expression on the two first dimensions, with the contribution of markers color-coded
1147 according to their cluster (top) and the distribution of samples grouped by treatment and
1148 temperature (bottom). Ellipses correspond to 95% confidence intervals around the
1149 centroid. Note that a single marker may be assigned to several clusters if the
1150 corresponding primer targets several homologous genes (Table S2).
1151
1152 **Fig. 8. The duration of heat exposure before ASM treatment moderately affects the**
1153 **dampening of ASM-induced transcriptional regulation.** Effect of heat duration prior to
1154 treatment on the expression of selected markers 3 d after ASM or water treatment, in
1155 grafted plants subjected to a 1-d, 2-d, 3-d and 4-d heatwave at 35°C. Expression values
1156 of water-treated leaves from plants exposed to 3-d 35°C were used for the calculation of
1157 the log_2 ratio. Expression values were obtained from 6 biological replicates equally from
1158 2 independent trials. **(a)** Schematic diagram of the experimental protocol. Air temperature
1159 during the contrasting thermal scenario (period in the growth chamber) is color-coded
1160 according to the color map. Arrows indicate the application of ASM (or water) treatment
1161 and the sampling of the youngest unfolded leaves. **(b)** Heatmap showing relative gene
1162 expression and ANOVA effect sizes (η^2_p) of treatment, temperature and their interaction,
1163 as well as their respective significance level (*P<0.05, **P<0.01, ***P<0.001,
1164 ****P<0.0001). **(c)** PCA representation of relative gene expression on the two first
1165 dimensions, with the contribution of markers color-coded according to their cluster (top)
1166 and the distribution of samples grouped by treatment and temperature (bottom). Ellipses
1167 correspond to 95% confidence intervals around the centroid. Note that a single marker
1168 may be assigned to several clusters if the corresponding primer targets several
1169 homologous genes (Table S2).

1170

1171 **Fig. 9. A heatwave posterior to ASM application dampens ASM-induced**
1172 **transcriptional regulation more strongly than a prior heatwave.** Effect of heatwave
1173 positioning on expression of selected markers 3 d after ASM or water treatment, in grafted
1174 plants subjected to a 3-d heatwave at 35°C before, during or after ASM or water treatment.
1175 Expression values of water-treated leaves from plants under heatwave during the
1176 treatment were used for the calculation of the $\log_2$ ratio. Expression values were obtained
1177 from 6 biological replicates equally from 2 independent trials. **(a)** Schematic diagram of
1178 the experimental protocol. Air temperature during the contrasting thermal scenario (period
1179 in the growth chamber) is color-coded according to the color map. Arrows indicate the
1180 application of ASM (or water) treatment and the sampling of the youngest unfolded leaves.
1181 **(b)** Heatmap showing relative gene expression and ANOVA effect sizes (η^2_p) of treatment,
1182 temperature and their interaction, as well as their respective significance level (*P<0.05,
1183 **P<0.01, ***P<0.001, ****P<0.0001). **(c)** PCA representation of relative gene expression
1184 on the two first dimensions, with the contribution of markers color-coded according to their
1185 cluster (top) and distribution of samples grouped by treatment and temperature (bottom).
1186 Ellipses correspond to 95% confidence intervals around the centroid. Note that a single
1187 marker may be assigned to several clusters if the corresponding primer targets several
1188 homologous genes (Table S2).

1189

1190 **Fig. 10. Working model for the loss of ASM-induced protection of apple plants upon**
1191 **transient heat.** At control temperature (20°C), spraying apple plants with ASM prior to
1192 inoculation with the bacteria *E. amylovora* or the fungus *V. inaequalis* allows apple leaves
1193 to mount an effective transcriptional response whereby resistance-associated genes are
1194 up-regulated and susceptibility-associated genes are down-regulated – which reduces the
1195 incidence of fire blight or apple scab. When a heatwave (35°C) occurs in between ASM
1196 application and pathogen inoculation, ASM-induced transcriptional regulation is
1197 dampened, ultimately enabling pathogens to proliferate. Created in BioRender.com.

1198

1199

1200 **Supplementary figures captions**

1201

1202 **Fig. S1. Climatic variables measured at the meteorological station of Beaucouzé**
1203 **(France) for the eleven hottest days recorded between March 2016 and July 2018.**
1204 Empty circles correspond to individual, hourly values. **(a)** Air temperature, **(b)** relative
1205 humidity (RH), **(c)** solar radiation and corresponding percent irradiance. Grey solid curves
1206 represent the average trend as determined by the non-parametric loess method (span =
1207 0.5), surrounded by the standard error (grey shaded area). Red dashed lines indicate the
1208 piecewise linear approximation of each climatic variable that was used to design the
1209 heatwave scenarios in the growth chamber.

1210

1211 **Fig. S2. Climate dynamics applied in the growth chamber to study the effect of**
1212 **heatwaves on apple response to ASM. (a)** "Control", **(b)** "Short" and **(c)** "Long"
1213 scenarios showing the daily variations in temperature, relative humidity (RH) and percent
1214 irradiance applied in growth chambers. Combination of these elemental daily programs
1215 were used to reproduce the different thermal scenarios that were studied.

1216

1217 **Fig. S3. Impact of heat and treatment on plant phenotype, and representative**
1218 **photographs of apple seedlings and their typical disease symptoms. (a)**, **(b)**, and **(c)**
1219 Boxplots and jitter plots showing the impact of temperature scenario and ASM or water
1220 treatment on apple seedling phenotypes. All measurements were performed on the same
1221 plants of the same experiment (Methods). At time 0, plants were sprayed with ASM or
1222 water and immediately transferred from a greenhouse to a growth chamber with controlled
1223 environmental conditions. Air temperature was maintained at either 20°C or 35°C for 24
1224 h, and all plants then remained in the growth chamber at 20°C during 48 h more. The
1225 elongation rate of **(a)** the stem and **(b)** the youngest unfolded leaf was calculated using
1226 measurements made before treatment and 3 d after treatment. Statistical differences
1227 between ASM and water treatment were determined at each temperature using pairwise
1228 t-tests adjusted by the Bonferroni method, and were deemed not significant (ns). **(c)**
1229 Stomatal conductance (g_s) was measured on the youngest unfolded leaf at time of
1230 ASM/water treatment application (left panel) and on the leaf rank immediately below (right
1231 panel), 1.5 h before treatment and 3, 48 and 72 h after treatment. Multiple mean

1232 comparisons were performed between each combination of both factors at each time point
1233 using pairwise t-tests adjusted by the Bonferroni method (* 0.05≥P>0.01, **
1234 0.01≥*P*>0.001). Note that non-significant differences have been omitted for clarity. **(d)**
1235 Photograph of a representative batch of apple seedlings at the start of the experiment. **(e)**
1236 Photograph of systemic fire blight necrosis symptoms on a diseased apple seedling, 21 d
1237 after inoculation by *E. amylovora*. The inoculated leaf is indicated by a white arrowhead
1238 and the picture focuses on necrotic symptoms spreading along the midvein of a distant
1239 leaf, and along the stem up to the plant apex. **(f)** Photograph of an apple seedling leaf
1240 showing *V. inaequalis* sporulation, 21 d after inoculation.
1241
1242 **Fig. S4. Accumulation of high temperatures prior to inoculation impairs the ability**
1243 **of apple grafts of GDDH13 to mount an effective ASM-induced protection against *E.***
1244 ***amylovora*. (a)** Schematic representation of the experimental protocol (details in
1245 Methods). Air temperature during the contrasting thermal scenario (period in the growth
1246 chamber) is color-coded according to the color map. Arrows indicate the application of
1247 ASM (or water) treatments and pathogen inoculation on the youngest unfolded leaf. **(b)**
1248 Stacked bar chart showing the proportion of healthy (asymptomatic on stem) and diseased
1249 (symptomatic on stem) grafted plants inoculated with *E. amylovora*, 28 d post-inoculation.
1250 Data represent 48 biological replicates from 4 independent trials (n = total number of
1251 plants). Statistical significance was determined using pairwise Fisher's exact tests; same
1252 letters indicate groups that are not significantly different. Icons created in BioRender.com.
1253 **(c)** Photograph of a diseased GDDH13 graft presenting fire blight symptoms on the apex
1254 and displaying the typical “hook shape”.
1255
1256 **Fig. S5. Identification of gene clusters by CAST.** Clustering was based on the
1257 expression pattern of 3108 genes that displayed differential expression (defined by a $|\log_2$
1258 $\text{ratio}| \geq 1$ and $P < 0.05$ in at least one microarray comparison, see Fig. 5b) in plants treated
1259 with ASM or water and exposed to control (21°C) or elevated (35°C) temperature. Pearson
1260 correlation distance metric (0.95 threshold affinity) allowed the construction of 26 clusters.
1261 Grey lines correspond to the expression ratio pattern of each individual DEG. Red points
1262 correspond to the average $\log_2$ expression ratio (± sd) within each comparison, for each

1263 cluster. The number of DEGs grouped in each cluster and the corresponding cluster
1264 number (and name for R1, R2, R3, S1 and S2 investigated in Fig. 6) are indicated in the
1265 upper right- and left-hand corner of each box, respectively.
1266
1267 **Fig. S6. Protection provided by ASM to apple seedlings against *E. amylovora* is**
1268 **more strongly dampened by a heatwave posterior to ASM application than by a**
1269 **prior heatwave.** (a) Schematic representation of the experimental protocol (details in
1270 Methods). Air temperature during the contrasting thermal scenario (period in the growth
1271 chamber) is color-coded according to the color map. Arrows indicate the application of
1272 ASM (or water) treatments and pathogen inoculation on the youngest unfolded leaf. (b)
1273 Stacked bar charts showing the proportion of healthy (asymptomatic on stem) and
1274 diseased (symptomatic on stem) seedlings inoculated with *E. amylovora* at 7, 14 and 21
1275 d post-inoculation (dpi). Data represent 55–56 biological replicates (number of plants in
1276 each condition) from a single trial. The *p*-value of Fisher's exact test between water and
1277 ASM treatments is shown above each pair of barplot (•P<0.1, *P<0.05). Icons created in
1278 BioRender.com.
1279
1280 **Fig. S7. Putative apple genes of SA biosynthesis pathway are induced by ASM at**
1281 **high temperature.** The expression pattern of putative apple orthologues of genes
1282 involved in SA biosynthesis was extracted from microarray data on GDDH13 leaves
1283 (Fig. 5). For each enzymatic step, expression of corresponding gene(s) are color-coded
1284 in boxes showing the effect of ASM ① at 21°C and ② at 35°C, and the effect of high
1285 temperature upon treatment with ③ water and ④ ASM. Significant up- or down-regulations
1286 are notified (*). The gene represented by grey boxes was absent from the microarray. (a)
1287 Phenylalanine ammonia-lyase (PAL) pathway. Apple protein orthologues of cinnamoyl-
1288 coenzyme A ligase (CNL) / *Oryza sativa* SA-DEFICIENT GENE 1 (OSD1), ABNORMAL
1289 INFLORESCENCE MERISTEM1 (AIM1), 3-ketoacyl-CoA thiolase (KAT), benzyl alcohol
1290 benzoyltransferase (BEBT) / OSD2, benzyl benzoate oxidase (BBO) / ODS3 /
1291 benzylbenzoate hydroxylase (BBH) and benzyl salicylate hydrolase (BSH) / OSD4 /
1292 benzylsalicylate esterase (BSE) were identified according to a BLAST of protein sequence
1293 from rice. Apple protein with an e-value of 0, less than 10% of gaps and 60% of identities

1294 were retained. If no protein met these criteria, the top four hits were selected. (b)
1295 Isochorismate synthase (ICS) pathway. Apple mRNA orthologues of ICS, AVRPPHB
1296 SUSCEPTIBLE 3 (PBS3) and ENHANCED PSEUDOMONAS SUSCEPTIBILITY 1
1297 (EPS1) were identified according to a BLAST with at least 60% of identities with CDS
1298 sequence from *Arabidopsis thaliana*.
1299
1300
1301 **Supplementary tables captions**
1302
1303 **Table S1. List of genes that are differentially regulated by ASM treatment and**
1304 **transient heat according to the microarray analysis.** Differentially expressed genes
1305 were defined by a $|\log_2 \text{ratio}| \geq 1$ and $P < 0.05$. The table shows gene accession, gene
1306 description, gene symbol (if any), $\log_2$ fold change within each comparison, cluster
1307 membership (see Fig. S5), and functional annotation. Gene description and functional
1308 annotation are based on the GDDH13 genome annotation (Daccord *et al.*, 2017).
1309
1310 **Table S2. Design of "resistance" and "susceptibility" marker genes.** Genes initially
1311 selected through CAST belonged to "resistance" (R1, R2, R3) or "susceptibility" (S1, S2)
1312 clusters (Fig. 6). Homologous genes were searched in the genome, and were eventually
1313 found in the same or an alternative cluster. Primers were designed to target as many
1314 homologous genes as possible, and the targeted ones are bolded. The table shows gene
1315 name, functional annotation, accession, cluster membership (if any), and primer sequence
1316 and concentration. Functional annotation is based on the GDDH13 genome annotation
1317 (Daccord *et al.*, 2017).

Figure 1

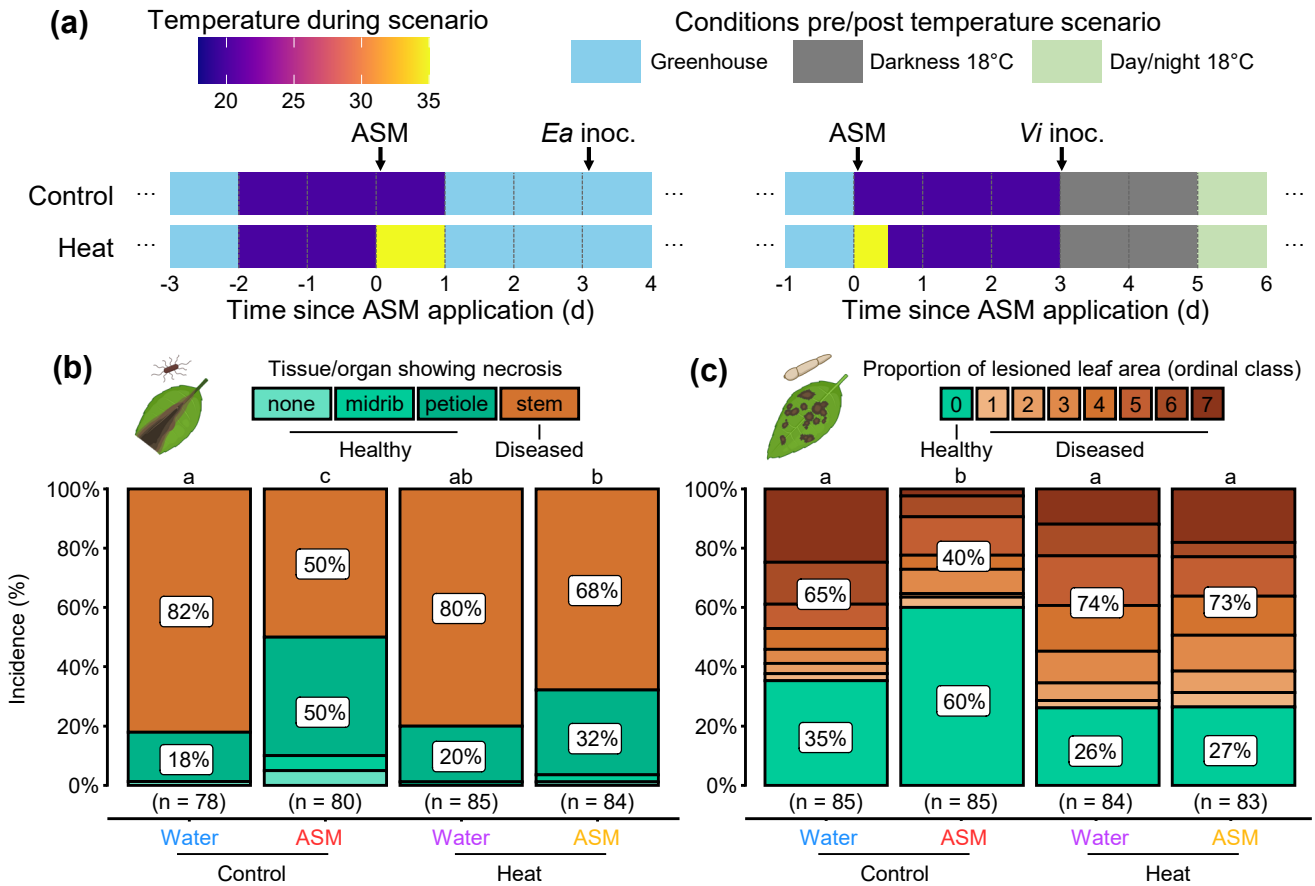

Fig. 1. Protection provided by ASM to apple seedlings against *E. amylovora* and *V. inaequalis* is impaired by transient exposure to heat. (a) Schematic representation of the experimental protocol applied to plants for *E. amylovora* (left) and *V. inaequalis* (right) disease assessment (details in Methods). Air temperature during the contrasting thermal scenario (period in the growth chamber) is color-coded according to the color map. Arrows indicate the application of ASM (or water) treatment and pathogen inoculation on the youngest unfolded leaf. **(b)** Stacked bar chart showing the proportion of healthy (asymptomatic on stem) and diseased (symptomatic on stem) seedlings inoculated with *E. amylovora*, 21 d post-inoculation. **(c)** Stacked bar chart showing the proportion of healthy (no visible sporulation) and diseased (visible sporulation) seedlings inoculated with *V. inaequalis*, 21 d post-inoculation. Data represent 78 to 85 biological replicates from 2 independent trials for each pathogen (n = total number of plants). Statistical significance was determined using pairwise Fisher's exact tests; same letters indicate groups that are not significantly different. Icons created in BioRender.com.

Figure 2

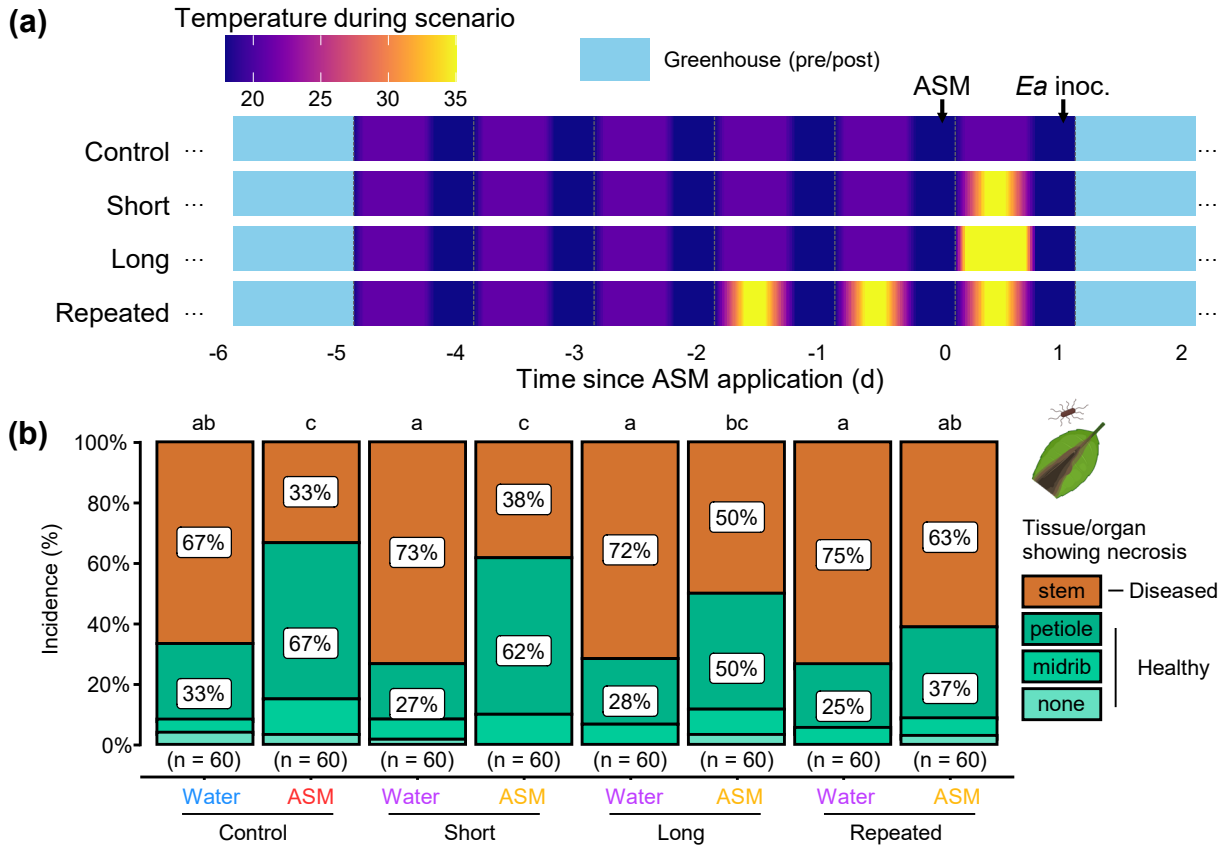

Fig. 2. Accumulation of high temperatures prior to inoculation impairs the ability of apple seedlings to mount an effective ASM-induced protection against *E. amylovora*. (a) Schematic representation of the experimental protocol (details in Methods). Air temperature during the contrasting thermal scenario (period in the growth chamber) is color-coded according to the color map. Arrows indicate the application of ASM (or water) treatment and pathogen inoculation on the youngest unfolded leaf. **(b)** Stacked bar chart of seedlings showing the proportion of healthy (asymptomatic on stem) and diseased (symptomatic on stem) seedlings inoculated with *E. amylovora*, 21 d post-inoculation. Data represent 60 biological replicates from 3 independent trials (n = total number of plants). Statistical significance was determined using pairwise Fisher's exact tests; same letters indicate groups that are not significantly different. Icons created in BioRender.com.

Figure 3

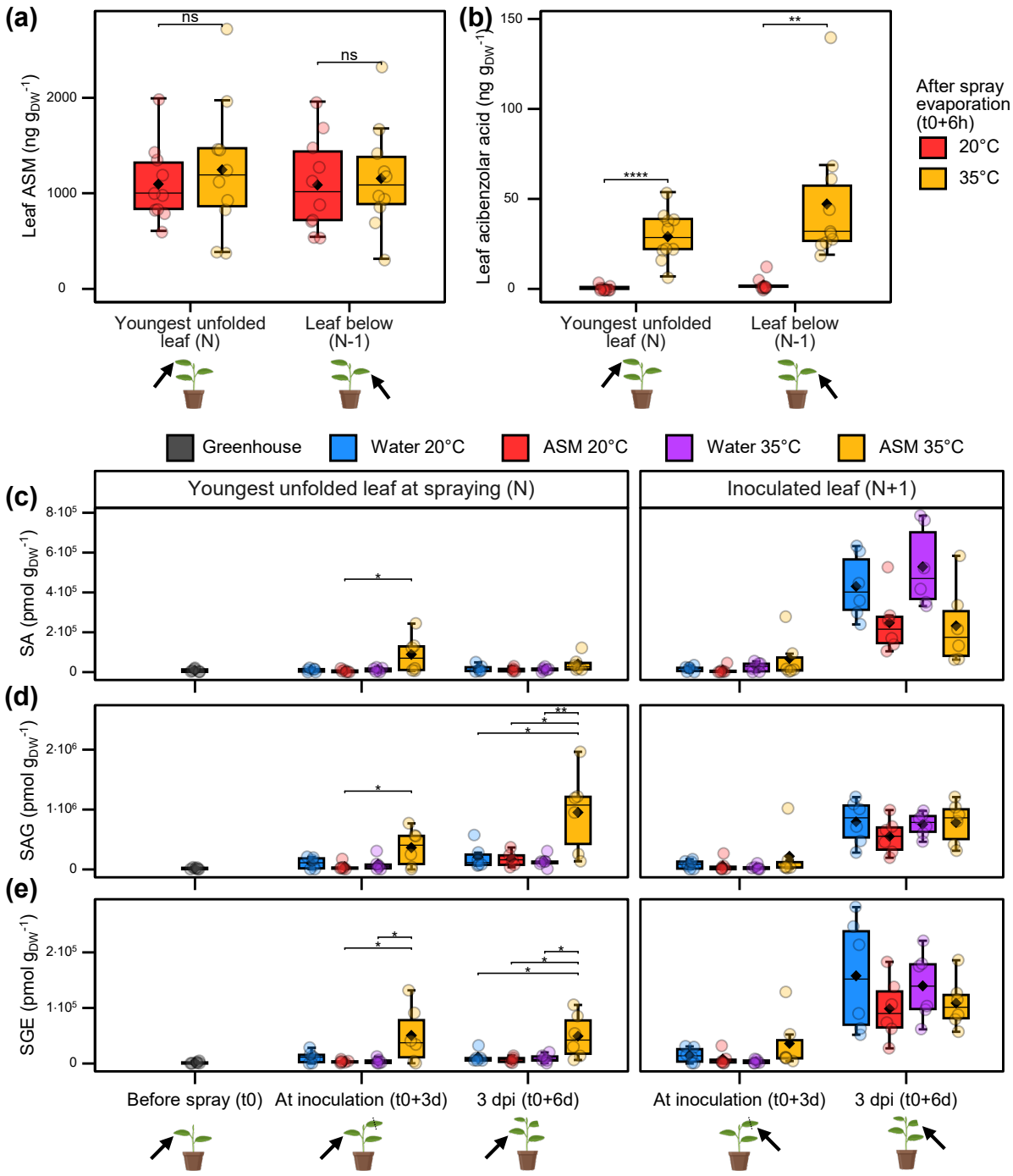

Fig. 3. High temperature does not alter ASM uptake or SA metabolism in apple seedlings. (a) and **(b)** Content of ASM and acibenzolar acid (biologically-active catabolite) in the lamina of ASM-treated leaves (n = 10, each pooled from 2 different plants). Apple seedlings were sprayed with ASM (t_0) and immediately transferred into a chamber at 20°C or 35°C. The youngest fully unfolded leaf (rank N) and the leaf below (rank N-1) were sampled after 6 h (when the sprayed solution had evaporated) and thoroughly rinsed before quantification of **(a)** ASM and **(b)** acibenzolar acid. **(c)**, **(d)** and **(e)** Content of salicylates in the lamina of water- or ASM-treated leaves (n = 6, each pooled from 8 different plants). Apple seedlings were sprayed with water or ASM (t_0) and immediately transferred into a chamber at 20°C or 35°C for 24 h, before being placed in a greenhouse. Three days after spraying (t_0+3d), half of the plants was sampled for the youngest fully unfolded leaf at time of spraying (rank N) and the leaf above (rank N+1), while the other half was inoculated with *E. amylovora* at leaf N+1. At three days post-inoculation (3 dpi, t_0+6d), the inoculated leaf N+1 and leaf N were harvested. A batch of plants was also harvested for leaf N just before t_0, in the greenhouse where the seedlings were grown. The samples were quantified for **(c)** salicylic acid (SA), **(d)** SA glucoside (SAG) and **(e)** SA glucose ester (SGE). ns: not significant, *: P<0.05, **: P<0.01, ***: P<0.001, ****: P<0.0001.

Figure 4

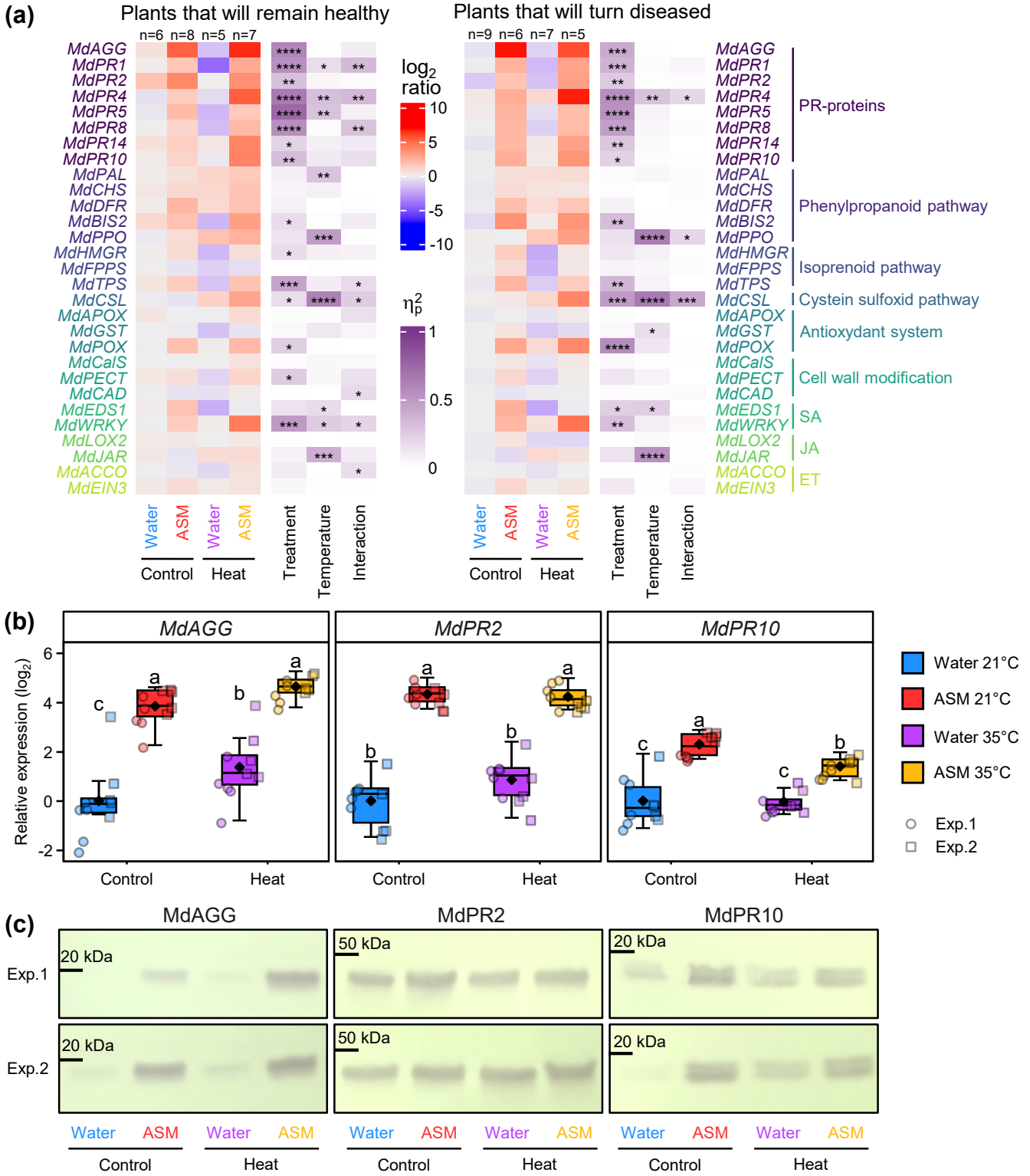

Fig. 4. High temperature does not prevent ASM-induction of defense markers. (a) Retrospective transcriptional analysis of 29 marker genes covering a broad range of apple defense mechanisms. Following a scenario similar as in Fig. 1a, young leaves of apple seedlings were individually sampled while inoculating with *E. amylovora*, and grouped *a posteriori* depending on the healthy or diseased fate of their corresponding plant. Heatmaps show relative gene expression and ANOVA effect sizes (η^2_p) of treatment, temperature and their interaction, as well as their respective significance level (*P<0.05, **P<0.01, ***P<0.001, ****P<0.0001), for both types of plants. Expression values of the average of water-treated leaves from healthy and diseased plants exposed to 20°C were used for the calculation of the $\log_2$ ratio. Expression values were obtained from 5–9 biological replicates (pools of 2 to 4 youngest unfolded leaves at time of ASM or water treatment) from a single trial. **(b)** Relative expression of *MdAGG*, *MdPR2* and *MdPR10* from two independent experiments performed in the same conditions as in Fig. 5a (3-d heatwave, GDDH13 grafted plants – see afterwards). The youngest unfolded leaf at time of sampling was collected from 5 plants per experiment. **(c)** Protein immunodetection of defense-associated proteins. Equal quantities (10 µg) of each protein sample were loaded and run in three separate SDS-PAGE gels. Following transfer to PVDF membranes, each blot was probed with the appropriate primary antibody to detect MdAGG, MdPR2, and MdPR10. Each sample corresponds to a pool of proteins extracted from the 5 biological replicates per experiment presented in **(b)**.

Figure 5

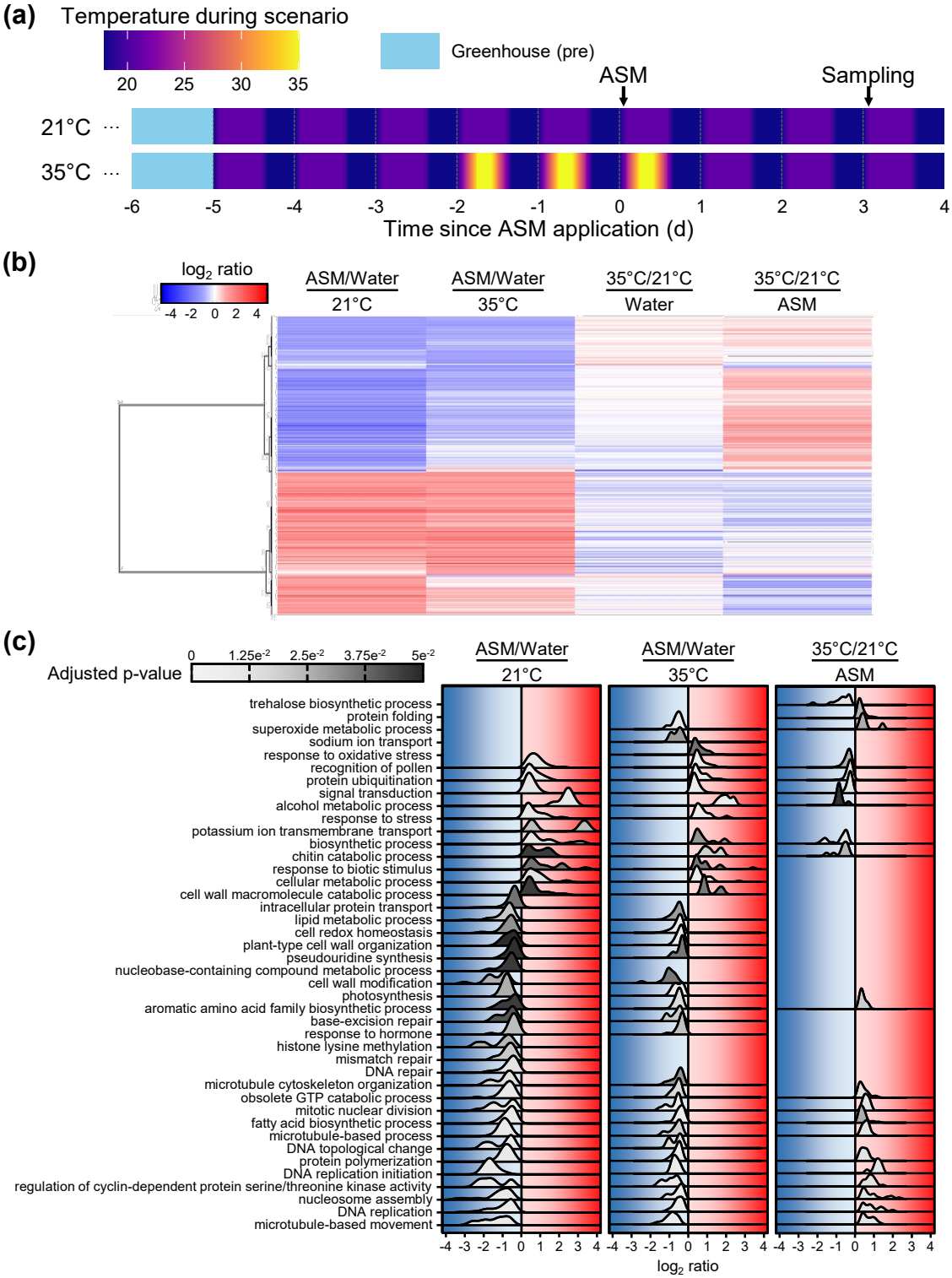

Fig. 5. High temperature dampens transcriptomic response to ASM but does not repress global defense. (a) Schematic diagram of the experimental protocol. Air temperature during the contrasting thermal scenario (period in the growth chamber) is color-coded according to the color map. Arrows indicate the application of ASM or water treatment and the sampling of the youngest unfolded leaf of GDDH13 grafted plants dedicated to microarray analysis. **(b)** Heatmap of 3108 DEGs identified in at least one microarray comparison. DEGs were defined by a $|\log_2 \text{ratio}| \geq 1$ and $P < 0.05$. The hierarchical clustering dendrogram was constructed from the dissimilarity matrix. Expression values were obtained from 2 biological replicates (each pooled from the youngest fully expanded leaf of 4 grafted plants) from 2 independent trials. **(c)** Ridgeline plot of GSEA on biological process ontology performed on comparison ASM/water for plants exposed to both 21°C and 35°C and 35°C/21°C comparison for ASM-treated plants. GSEA was obtained by 10.000 permutations with Benjamini and Hochberg procedure for p-value adjustment.

Figure 6

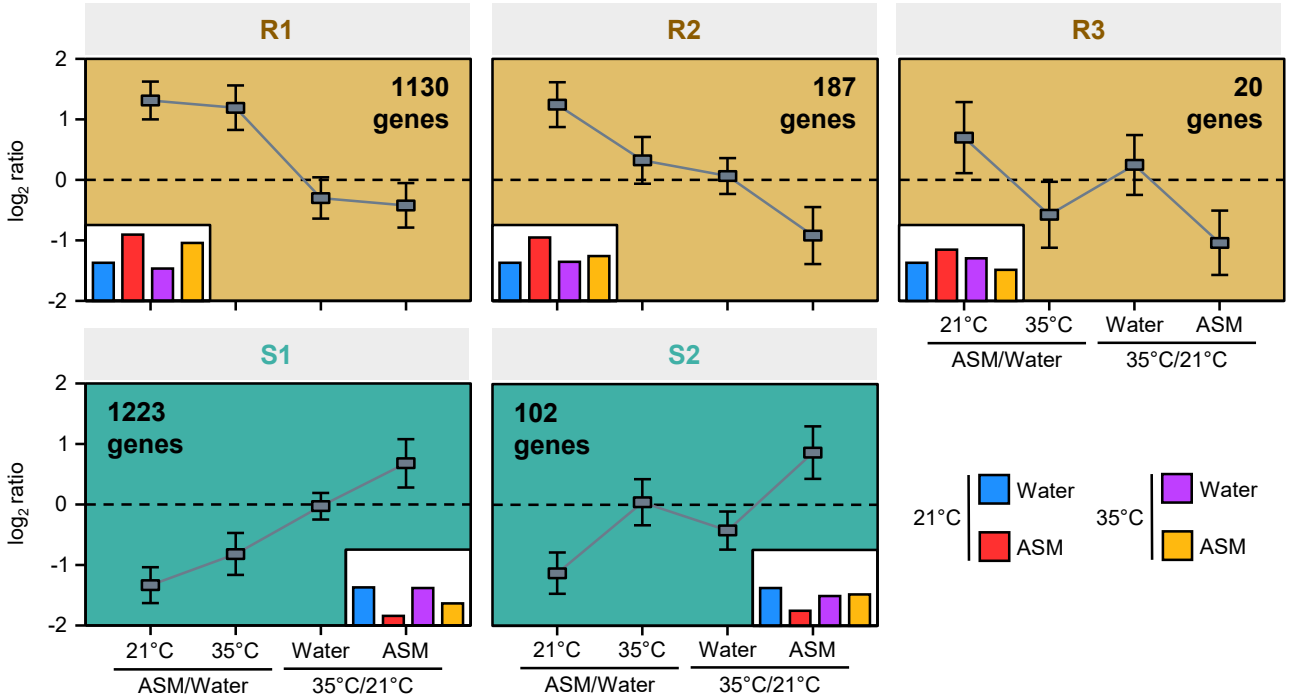

Fig. 6. Identification of "resistance-associated" and "susceptibility-associated" marker genes by clustering. CAST clustering performed on the 3108 DEGs (Table S1 and Fig. S5) yielded several clusters evocative of resistant (R1, R2 and R3) and susceptible (S1 and S2) marker genes. The average pattern of expression ratio (± sd) is shown for each cluster. The number of DEGs in each resistance or susceptibility cluster are indicated in the upper right- or left-hand corner, respectively. To facilitate the interpretation of the variations in ratios, barplots showing the inferred expression pattern relative to the control (water, 21°C) are placed in the lower left- or right-hand corner of resistance and susceptibility clusters, respectively.

Figure 7

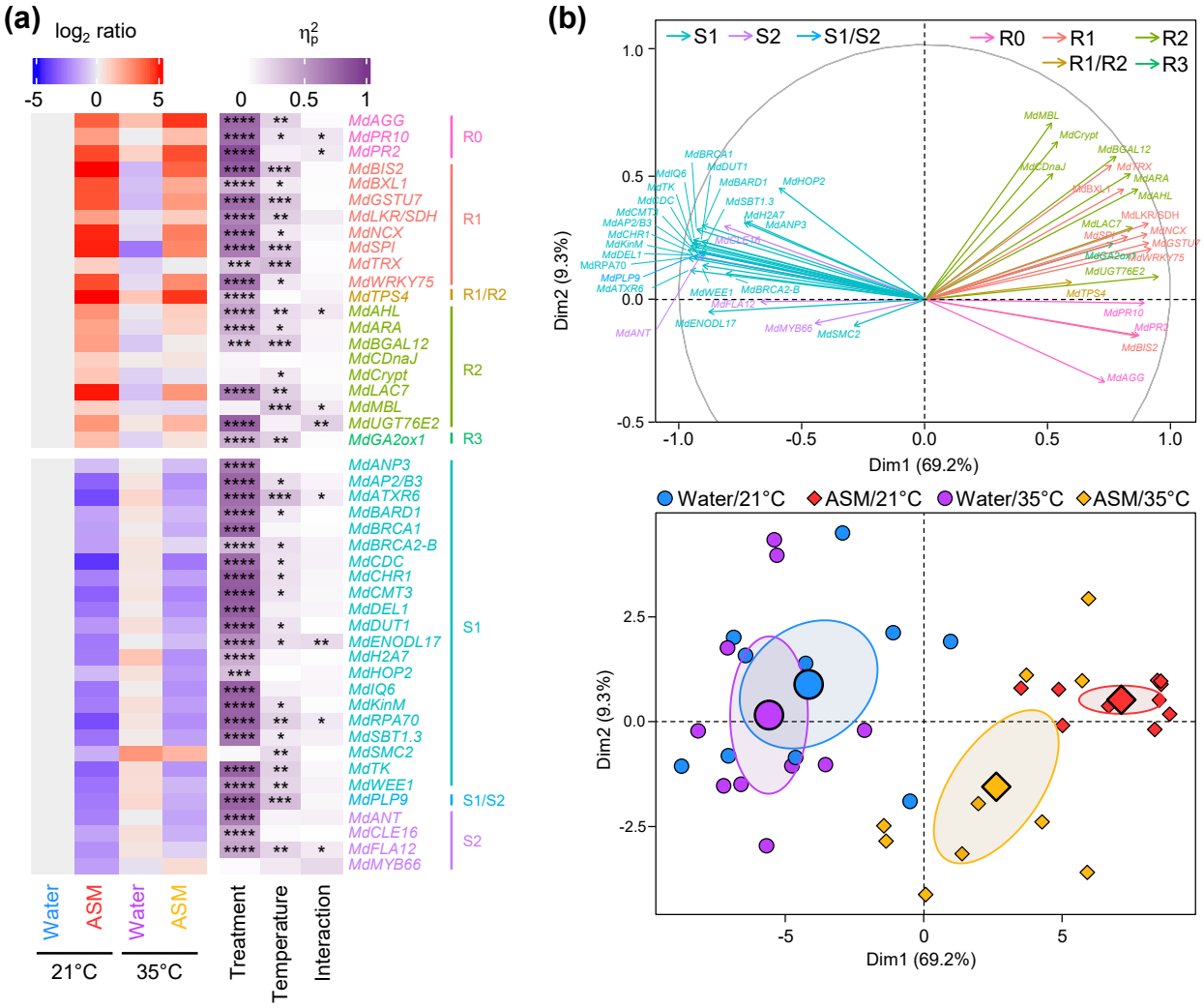

Fig. 7. High temperature erodes ASM-induced transcriptional regulation of resistance- and susceptibility-associated marker genes. Expression values of water-treated leaves from plants exposed to 21°C were used for the calculation of the $\log_2$ ratio. Expression values were obtained from 10 biological replicates equally from 2 independent trials. **(a)** Heatmap showing relative gene expression and ANOVA effect sizes (η^2_p) of treatment, temperature and their interaction, as well as their respective significance level (*P<0.05, **P<0.01, ***P<0.001, ****P<0.0001). **(b)** PCA representation of relative gene expression on the two first dimensions, with the contribution of markers color-coded according to their cluster (top) and the distribution of samples grouped by treatment and temperature (bottom). Ellipses correspond to 95% confidence intervals around the centroid. Note that a single marker may be assigned to several clusters if the corresponding primer targets several homologous genes (Table S2).

Figure 8

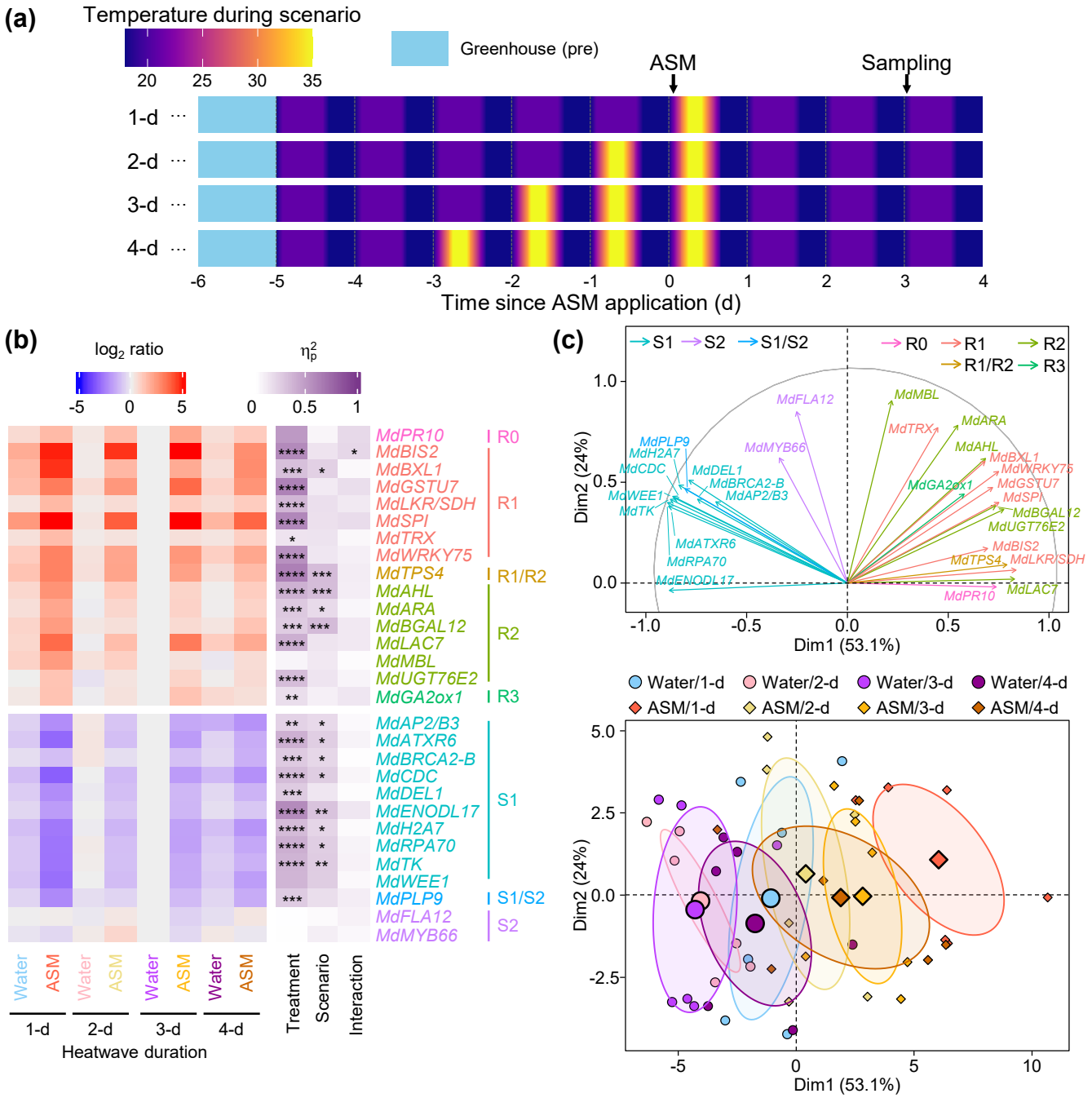

Fig. 8. The duration of heat exposure before ASM treatment moderately affects the dampening of ASM-induced transcriptional regulation. Effect of heat duration prior to treatment on the expression of selected markers 3 d after ASM or water treatment, in grafted plants subjected to a 1-d, 2-d, 3-d and 4-d heatwave at 35°C. Expression values of water-treated leaves from plants exposed to 3-d 35°C were used for the calculation of the $\log_2$ ratio. Expression values were obtained from 6 biological replicates equally from 2 independent trials. **(a)** Schematic diagram of the experimental protocol. Air temperature during the contrasting thermal scenario (period in the growth chamber) is color-coded according to the color map. Arrows indicate the application of ASM (or water) treatment and the sampling of the youngest unfolded leaves. **(b)** Heatmap showing relative gene expression and ANOVA effect sizes (η^2_p) of treatment, temperature and their interaction, as well as their respective significance level (*P<0.05, **P<0.01, ***P<0.001, ****P<0.0001). **(c)** PCA representation of relative gene expression on the two first dimensions, with the contribution of markers color-coded according to their cluster (top) and the distribution of samples grouped by treatment and temperature (bottom). Ellipses correspond to 95% confidence intervals around the centroid. Note that a single marker may be assigned to several clusters if the corresponding primer targets several homologous genes (Table S2).

Figure 9

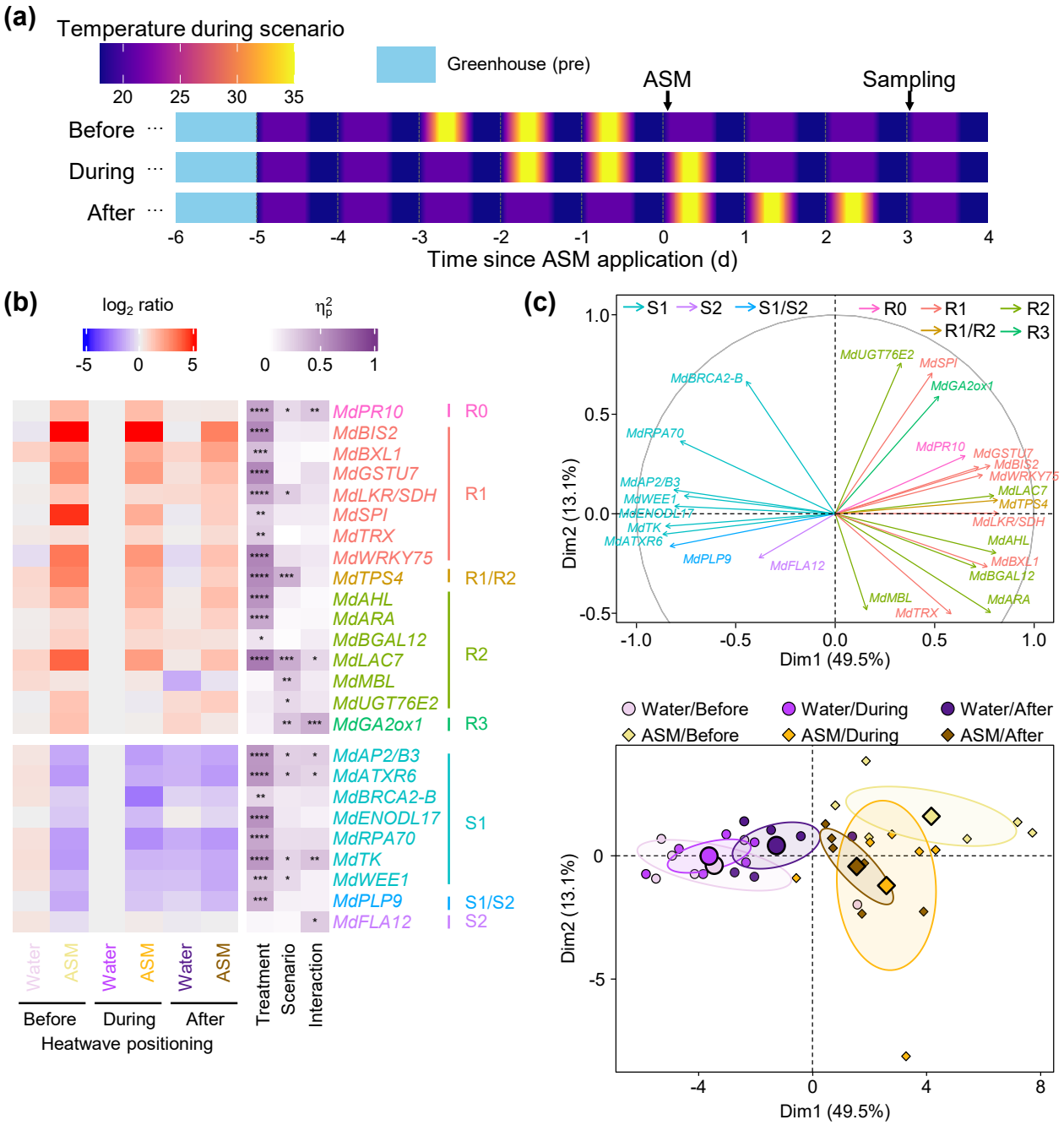

Fig. 9. A heatwave posterior to ASM application dampens ASM-induced transcriptional regulation more strongly than a prior heatwave. Effect of heatwave positioning on expression of selected markers 3 d after ASM or water treatment, in grafted plants subjected to a 3-d heatwave at 35°C before, during or after ASM or water treatment. Expression values of water-treated leaves from plants under heatwave during the treatment were used for the calculation of the $\log_2$ ratio. Expression values were obtained from 6 biological replicates equally from 2 independent trials. **(a)** Schematic diagram of the experimental protocol. Air temperature during the contrasting thermal scenario (period in the growth chamber) is color-coded according to the color map. Arrows indicate the application of ASM (or water) treatment and the sampling of the youngest unfolded leaves. **(b)** Heatmap showing relative gene expression and ANOVA effect sizes (η^2_p) of treatment, temperature and their interaction, as well as their respective significance level (*P<0.05, **P<0.01, ***P<0.001, ****P<0.0001). **(c)** PCA representation of relative gene expression on the two first dimensions, with the contribution of markers color-coded according to their cluster (top) and distribution of samples grouped by treatment and temperature (bottom). Ellipses correspond to 95% confidence intervals around the centroid. Note that a single marker may be assigned to several clusters if the corresponding primer targets several homologous genes (Table S2).

Figure 10

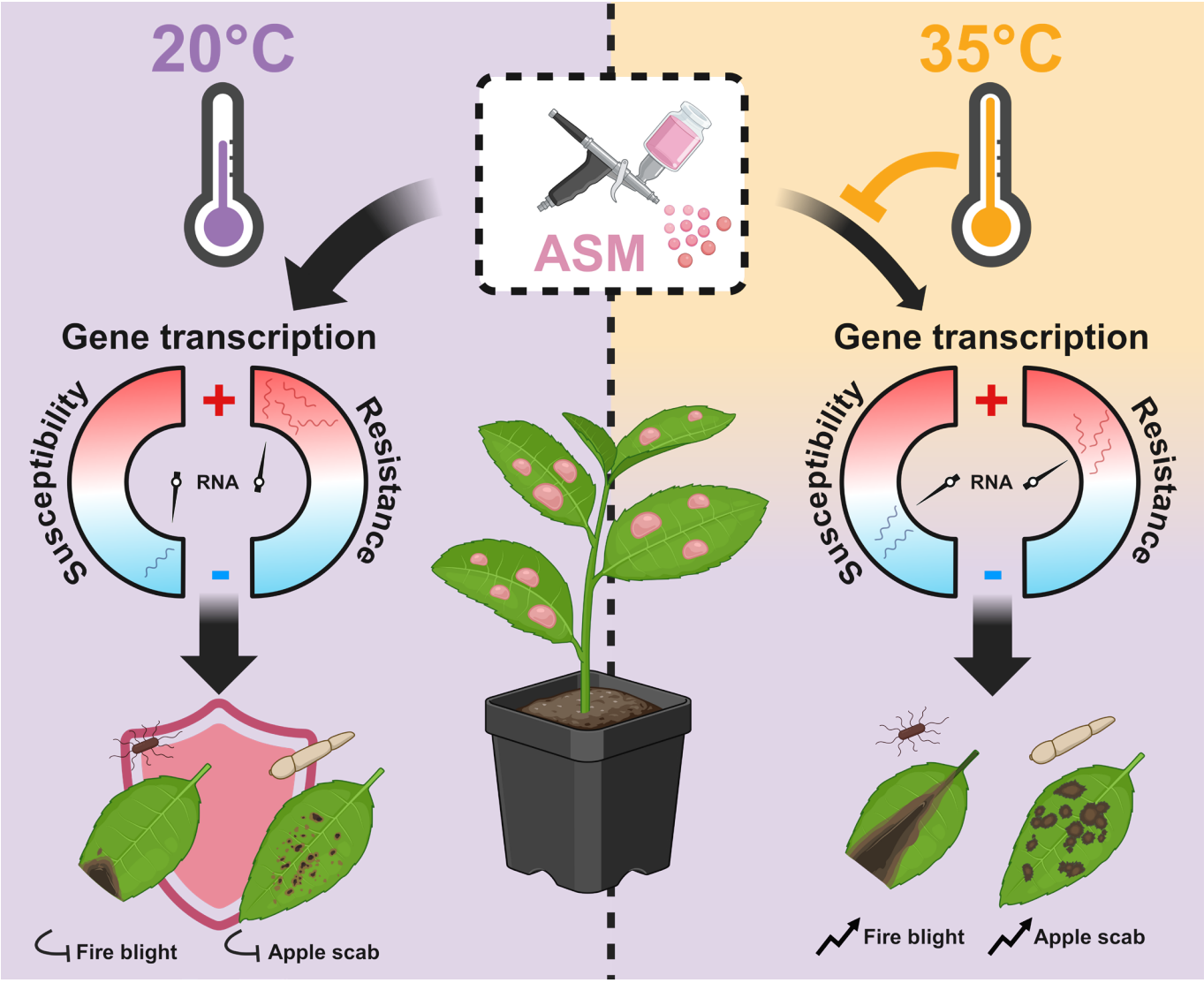

Fig. 10. Working model for the loss of ASM-induced protection of apple plants upon transient heat. At control temperature (20°C), spraying apple plants with ASM prior to inoculation with the bacteria *E. amylovora* or the fungus *V. inaequalis* allows apple leaves to mount an effective transcriptional response whereby resistance-associated genes are up-regulated and susceptibility-associated genes are down-regulated – which reduces the incidence of fire blight or apple scab. When a heatwave (35°C) occurs in between ASM application and pathogen inoculation, ASM-induced transcriptional regulation is dampened, ultimately enabling pathogens to proliferate. Created in BioRender.com.